NASA TECHNICAL NOTE

NASA TN D-5046

C. 1

TECH LIBRARY KAFB, NM
0131937

NASA TN D-5046

LOAN COPY: RETURN TO
AFWL (WLIL-2)
KIRTLAND AFB, N MEX

A METHOD FOR DETERMINING THE TOTAL DRAG OF A POINTED BODY OF REVOLUTION IN SUPERSONIC FLOW WITH TURBULENT BOUNDARY LAYER

by Charlie M. Jackson, Jr., and Rudeen S. Smith

Langley Research Center
Langley Station, Hampton, Va.

NATIONAL AERONAUTICS AND SPACE ADMINISTRATION • WASHINGTON, D. C. • MARCH 1969

TECH LIBRARY KAFB, NM
0131937

A METHOD FOR DETERMINING THE TOTAL DRAG OF A POINTED BODY OF REVOLUTION IN SUPERSONIC FLOW WITH TURBULENT BOUNDARY LAYER

By Charlie M. Jackson, Jr., and Rudeen S. Smith

Langley Research Center
Langley Station, Hampton, Va.

NATIONAL AERONAUTICS AND SPACE ADMINISTRATION

For sale by the Clearinghouse for Federal Scientific and Technical Information
Springfield, Virginia 22151 – CFSTI price $3.00

A METHOD FOR DETERMINING THE TOTAL DRAG OF A POINTED BODY OF REVOLUTION IN SUPERSONIC FLOW WITH TURBULENT BOUNDARY LAYER

By Charlie M. Jackson, Jr., and Rudeen S. Smith
Langley Research Center

SUMMARY

An approximate mathematical model of the inviscid and viscid flow field about a body of revolution has been developed by utilizing modifications of the second-order shock-expansion theory and of a theoretical analysis of compressible boundary-layer growth with pressure gradient. The area of application of this model is intended to be restricted to the attached bow-shock condition in the supersonic flow region with an all-turbulent boundary layer. The viscid-inviscid interaction is accounted for by iteration between the respective theories. The solution of the mathematical model including the iteration and the integration of surface conditions to give wave and friction drags has been programed for digital computation, and the program is included herein.

The inviscid solution is shown to compare well with the method of characteristics for a wide range of body shapes including local surface compressions and moderate amounts of boattail. The basic theory has been extended to provide an estimate of the flow-field pressures and shock shape.

The viscid solution in its simplified flat-plate and conical forms is demonstrated to agree well with the established flat-plate and cone solutions for a turbulent boundary layer. The theoretical estimates of the local skin friction were in good agreement with experiment for a body with moderate pressure gradient; even for a condition of strong favorable and adverse gradients on the same body, fair agreement was indicated.

The viscid and inviscid solutions including interactions were applied to several body shapes over a wide range of test conditions and the resulting total-drag estimates generally agreed with the reported experimental values to within 5 percent. In view of the difficulty involved in obtaining precise experimental data, it is believed that the present method is generally as accurate as the current experimental testing techniques.

INTRODUCTION

Currently many theoretical methods are available for predicting the viscid and inviscid drag forces on bodies of revolution. Most of these methods are based on assumptions which restrict the area of applicability. In the past two decades the effort expended on the development of drag prediction techniques has been primarily directed toward slender configurations. Engineering estimates can be obtained for the total drag of slender bodies of revolution in the low supersonic speed range with relatively little effort by applying one of the methods based on linear theory such as the supersonic area rule of reference 1 to obtain the wave drag and by using the turbulent-boundary-layer flat-plate friction analysis of reference 2 to obtain the friction drag. As the Mach number increases or the body slenderness decreases – that is, as the hypersonic similarity parameter (ratio of the free-stream Mach number to the fineness ratio of the body) increases – the results obtained from these methods become unreliable. A need therefore exists for a reliable method with which an engineer can, with relative ease, obtain estimates of the total drag of bodies of revolution over a wider range of conditions.

There are, of course, well-documented theories capable of accurately predicting the wave drag of bodies of revolution at high values of the hypersonic similarity parameter (refs. 3 and 4) and theoretical turbulent-boundary-layer analyses capable of providing accurate estimates of the boundary-layer growth and skin-friction drag (refs. 5 and 6). The purpose of the present work is to modify and combine the most promising of these theories to obtain a mathematical model of the viscid and inviscid flow field with sufficient detail to account for the most important interaction effects.

In the present paper the mathematical model is developed by using a modified form of the second-order shock-expansion theory of reference 3 to define the inviscid flow field. The turbulent-boundary-layer growth characteristics are obtained from a modification of the theory of reference 5, and an iteration technique is used to provide the final viscid and inviscid flow field from which the total drag is obtained. For convenience, the method is programed for the Control Data 6600 computer system and the program listing is included.

SYMBOLS

A	cross-sectional area of body
a	sonic velocity
a^*	sonic velocity at T^*

C_D drag coefficient, $\frac{\text{Drag}}{q_\infty A_{max}}$

C_F average coefficient of friction based on body surface area and free-stream conditions

C_p pressure coefficient, $\frac{p_w - p_\infty}{q_\infty}$

c_f local coefficient of friction based on free-stream conditions

FR fineness ratio

f friction term defined by equation (A5)

K slope of conical surface

l total body or flat-plate length

M Mach number

N velocity profile index (N = 7 in present analysis)

n constant (n = 1 for laminar flow; n = 1/6 for turbulent flow)

p static pressure

q dynamic pressure

R transformed body radius

R_g gas constant

R_∞ unit Reynolds number based on free-stream conditions

$R_{\infty,l}$ free-stream Reynolds number based on body length

r local body radius

S	transformed longitudinal distance along body surface from nose
s	longitudinal distance along body surface from nose
T	temperature
T^*	reference temperature
u	velocity
x	longitudinal coordinate (on body center line)
y	radial coordinate (origin at body center line)
Y'	transformed radial coordinate (origin at body surface)
y'	radial coordinate (origin at body surface)
α	shock angle (see eq. (1))
γ	ratio of specific heats, 1.4 for present analysis
δ	boundary-layer thickness
δ^*	displacement thickness, $\int_0^{\delta}\left(1 - \frac{\rho u}{\rho_e u_e}\right)\left(1 + \frac{y'}{r}\right)dy'$
δ^{**}	streamline displacement due to boundary layer (see eq. (17))
ϵ	half-angle of conical frustum body element
η	entropy
θ	momentum thickness, $\int_0^{\delta}\frac{\rho u}{\rho_e u_e}\left(1 - \frac{u}{u_e}\right)\left(1 + \frac{y'}{r}\right)dy'$
μ	absolute viscosity
ν	kinematic viscosity, μ/ρ

ρ	density

Subscripts:

base	model base
c	cone
e	conditions at edge of boundary layer
exp	experimental
i	incompressible
inv	inviscid
lam	laminar
max	maximum
T	transition point
t	stagnation conditions at edge of boundary layer
turb	turbulent
w	wall
∞	free-stream conditions

A bar over a quantity refers to flat-plate conditions.

THEORETICAL METHOD

The purpose of the present paper is to develop a mathematical model of the viscid and inviscid flow in the region of the surface of a body of revolution. This model is constructed with a view to providing an accurate total-drag prediction technique for arbitrary

bodies of revolution in the supersonic speed range with turbulent boundary layers. In order to construct the model, it is necessary to provide an inviscid solution and a viscid solution such that the two can be iterated to provide interaction effects. In the present paper these solutions are provided by modifying existing theories, as described in the following sections.

INVISCID SOLUTION

The inviscid solution of the present analysis is based on the second-order shock-expansion theory presented in reference 3. The details of the theory are well documented and are not discussed herein. Instead, a general description of the techniques used to employ the theory is given.

In order to apply the second-order shock-expansion theory, the body is represented by a series of cone frustums as shown schematically in figure 1. Also shown in figure 1 is a typical surface-pressure distribution obtained for the body by the second-order shock-expansion methods. The starting flow conditions at point 1 are based on the conical flow generated by the initial body section and may be obtained from the tables of reference 7. At the juncture of the initial cone and the first frustum element, the pressure change is determined by a Prandtl-Meyer expansion. The variation of the pressure on the frustum element from 2 to 3 in figure 1 is obtained by evaluating the first few terms of a series which would allow the surface pressure to approach conical pressure if the frustum were infinitely long. With this series, the pressure at 3 is obtained; then another Prandtl-Meyer expansion is used to obtain the pressure at 4; and so forth. The present technique is to divide the body into many frustums and base the body pressure distribution on the pressures at the midpoint of each element. An inherent difficulty with the second-order shock-expansion method is pointed out in reference 3. This difficulty arises at higher Mach numbers when the series which describes the pressure variation over an element becomes divergent. When this condition occurs, the present technique simply assumes the pressure to be constant over the element and equal to the value obtained after the expansion from the previous element.

When the second-order shock-expansion theory is applied to the boattail region of a body, the pressure series cannot be made to approach a conical value. In this region the present analysis requires the pressure series to approach a free-stream value at infinity, as suggested in reference 3. Figure 2 presents a comparison of the surface-pressure coefficient C_p determined from the present analysis (body represented by 20 cone frustums) with that determined by the method of characteristics for typical boattail bodies (Sears-Haack bodies) of fineness ratio 4 and 10 at $M_\infty = 2.0$. The results

presented in figure 2 indicate excellent agreement of the second-order shock-expansion theory with the method of characteristics except on the aft portion where the boattail angle exceeds 10^{o}.

Since the viscid solution of the present analysis will be based on inviscid conditions at the edge of the boundary layer, it is important that estimates of the pressure and Mach number be obtained in the region of the body surface. In order to conveniently provide these estimates, it has been assumed that the surface pressures and Mach numbers are propagated out from the surface along local Mach lines. For example, in figure 1 the surface pressure and Mach number in the region 1-3-b-a is assumed constant and equal to the surface pressure and Mach number at point 2-3. The boundaries of this region, lines 1-a and 3-b, are assumed to be Mach lines generated by the surface Mach numbers at points 1 and 3, respectively. Thus the angle of the boundary 1-a is $\sin^{-1}\frac{1}{M_1} + \epsilon_{0-1}$ and the angle of the boundary 3-b is $\sin^{-1}\frac{1}{M_3} + \epsilon_{2-3}$. The pressures and Mach numbers throughout the entire flow field, including the bow-shock shape, can be estimated with these assumptions. The shock angle can be determined for each constant-pressure element of the flow field from the equation

$$\alpha = \sin^{-1}\sqrt{\frac{6\frac{p}{p_\infty} + 1}{7M_\infty^{\,2}}} \tag{1}$$

An example of this procedure is shown in figure 1. In figure 1 the shock angle for the starting cone is obtained from the tables of reference 7 along with the surface Mach number. The surface Mach number is used to obtain the direction of the Mach line from the surface of the body at 1. The intersection of the starting cone shock with the Mach line from 1 defines the shock point a, from which the next shock element is constructed. The shock element from a to b is constructed at the angle α_{2-3} which is computed from equation (1), with the pressure behind the shock defined as the surface pressure p_{2-3}. In this manner the preliminary estimates of the shock shape and flow-field pressures are determined for the entire flow field.

In order to evaluate the estimates of the flow-field pressures and shock shape, results of the present method and the method of characteristics are compared in figure 3. In figure 3 the pressure coefficients are shown for Sears-Haack bodies of fineness ratios 4 and 10 at a free-stream Mach number of 2.0. Good agreement is indicated between the present method and the method of characteristics in the region of the body surface, with the exception of the aft portions of the body where high boattail angles occur. These results also indicate that the present method can be used to predict the shock shape and

forebody flow-field pressures to sufficient accuracy for preliminary interference analysis.

The second-order shock-expansion methods of reference 3 can be applied to bodies with local compressions, provided the compressions are small enough for the shock to be theoretically attached to the compression corner. The details of the calculating procedure for compression elements on the body surface are given in reference 3. The procedure essentially involves the use of the two-dimensional oblique shock relations at the start of the element and the evaluation of a series to provide the pressure variation over the element in the same manner as described for an expansion element. Reference 3 did not illustrate the use of the second-order shock-expansion theory on a body with local compression, so in order to evaluate the theory under these conditions, the pressure distribution on an inlet spike has been calculated by this method and compared with that calculated by the method of characteristics. This comparison is shown in figure 4 for a free-stream Mach number of 3.0. Figure 4 indicates good agreement between the theories for both the compression and the following expansion. For the present method the inlet spike of figure 4 was represented by 19 elemental cone frustums.

VISCID SOLUTION

The viscid solution of the present analysis consists of the use of the integral momentum equation in conjunction with a mathematical model of the turbulent boundary-layer growth. The present theory for determining the turbulent boundary-layer growth is based on a modification of the analysis of reference 5. The mathematical expression for the variation of the momentum thickness as developed in reference 5 is (in the notation of the present paper):

$$\theta = \frac{\left(1 + 0.2M_e^2\right)^3}{M_e^3 r}\left[\frac{0.0076\left(\frac{\nu_t}{a_t}\right)^{1/6}}{\left(1 + 0.2M_e^2\right)^{-5/42}}\int_0^s \frac{M_e^{10/3} r^{7/6}}{\left(1 + 0.2M_e^2\right)^4}\,ds\right]^{6/7} \tag{2}$$

Equation (2) is developed in reference 5 by extending the incompressible equation of reference 8 to the compressible condition by a transformation based on the work of reference 9. The analysis of reference 5 was slightly modified as indicated in appendix A, and equation (2) was rederived for the purposes of the present analysis to give

$$\theta = \frac{\left(1 + 0.2M_e^2\right)^3}{M_e^3 r}\left[\frac{0.0076\left(\frac{\nu_t}{a_t}\right)^{1/6}}{\left(1 + 0.2M_e^2\right)^{-11/42}}\int_0^s \frac{M_e^{10/3} r^{7/6}}{\left(1 + 0.2M_e^2\right)^4}\,ds\right]^{6/7} \tag{3}$$

A comparison of equation (3) with equation (2) indicates the net effect of the modifications of the present analysis to be the alteration of an exponent of a term in the denominator. This change has a tendency to increase the magnitude of the estimated value of the momentum thickness for specific inviscid conditions.

The effects of the modifications of the present analysis on the accuracy of the momentum-thickness expression of reference 5 are indicated in figure 5. Figure 5 shows the ratio of the momentum thickness calculated from equations (2) and (3) to the momentum thickness obtained from velocity profile measurements reported in references 10 and 11. In general, better agreement with the available data is indicated for the modified equation of the present analysis (eq. (3)) than for equation (2). Therefore, equation (3) is used herein.

A mathematical model of the turbulent boundary-layer growth on a body of revolution can be obtained on the basis of equation (3) with the additional assumption of an analytical form for the velocity profile. In the present analysis the well-known power-law profile is assumed to represent the velocity profile shape. Expressed in the present notation, the power-law profile is

$$\frac{u}{u_e} = \left(\frac{y'}{\delta}\right)^{1/N} \tag{4}$$

where the value of N is taken to be 7 for all conditions. The analysis of reference 12 incorporates equation (4) to provide expressions for the boundary-layer thickness and displacement thickness as functions of the momentum thickness on bodies of revolution. The expressions of reference 12, in the notation of the present paper, are

$$\frac{\theta}{\delta} = \frac{N}{2} \frac{T_e/T_t}{\left(1 - \frac{T_e}{T_t}\right)^{\frac{N+1}{2}}} \left[2 - \ln\left(\frac{T_e}{T_t}\right) + \frac{1}{\sqrt{1 - \frac{T_e}{T_t}}} \ln\left(\frac{1 - \sqrt{1 - \frac{T_e}{T_t}}}{1 + \sqrt{1 - \frac{T_e}{T_t}}} \right) - \sum_{i=1}^{\frac{N-1}{2}} \frac{\left(1 - \frac{T_e}{T_t}\right)^i}{i(2i+1)} \right]$$

$$+ \frac{\delta}{r} \frac{N}{2} \frac{T_e/T_t}{\left(1 - \frac{T_e}{T_t}\right)^N} \left[\frac{\ln\left(\frac{T_e}{T_t}\right)}{1 - \frac{T_e}{T_t}} - \frac{1}{\sqrt{1 - \frac{T_e}{T_t}}} \ln\left(\frac{1 - \sqrt{1 - \frac{T_e}{T_t}}}{1 + \sqrt{1 - \frac{T_e}{T_t}}} \right) - \sum_{i=0}^{N-1} \frac{\left(1 - \frac{T_e}{T_t}\right)^i}{(i+1)(2i+1)} \right] \tag{5}$$

and

$$\frac{\delta^*}{\delta} = 1 + \frac{1}{2}\frac{\delta}{r} + \frac{N}{2}\frac{T_e/T_t}{\left(1 - \frac{T_e}{T_t}\right)^{\frac{N+1}{2}}}\left[\sum_{i=1}^{\frac{N-1}{2}} \frac{\left(1 - \frac{T_e}{T_t}\right)^i}{i} + \ln\left(\frac{T_e}{T_t}\right)\right]$$

$$+ \frac{\delta}{r} N \frac{T_e/T_t}{\left(1 - \frac{T_e}{T_t}\right)^N}\left[\sum_{i=0}^{N-1} \frac{\left(1 - \frac{T_e}{T_t}\right)^i}{2i+1} - \frac{1}{2\sqrt{1 - \frac{T_e}{T_t}}} \ln \frac{1 + \sqrt{1 - \frac{T_e}{T_t}}}{1 - \sqrt{1 - \frac{T_e}{T_t}}}\right] \tag{6}$$

In the present analysis equations (5) and (6) are used in conjunction with the momentum thickness obtained from equation (3). By an iteration process the boundary-layer parameters δ, δ^*, and θ are obtained as functions of the body radius and inviscid flow conditions at the edge of the boundary layer. In order to start the iteration the initial values of θ/δ are taken to be those presented in the tables of reference 13 for two-dimensional boundary layers.

The local skin friction can be obtained from the variation of the boundary-layer parameters provided by the expressions of equations (3), (5), and (6) and the momentum equation. The form of the von Kármán integral momentum equation appropriate to bodies of revolution with pressure gradient is

$$\frac{c_f}{2}\frac{q_\infty}{q_e} = \frac{d\theta}{ds} + \theta\left[\frac{1}{r}\frac{dr}{ds} + \frac{2 - M_e^2 + \frac{\delta^*}{\theta}}{M_e\left(1 + 0.2M_e^2\right)}\frac{dM_e}{ds}\right] \tag{7}$$

Before considering the details of the solution of the boundary-layer equations for an arbitrary body with pressure gradient, it would be interesting to examine the expressions of the present analysis for flat-plate and conical flows for which closed-form solutions are available. Equations (3) and (7) can easily be reduced to flat-plate conditions by setting $M_e = M_\infty$ and $q_e = q_\infty$ and by letting $r \to \infty$. The following results for the flat-plate momentum thickness and local skin-friction variations are obtained:

$$\bar{\theta} = \frac{0.0152 s^{6/7}}{\left(1 + 0.2M_\infty^2\right)^{0.418} R_\infty^{1/7}}\left(\frac{T_\infty + 216}{T_t + 216}\right)^{1/7} \tag{8}$$

$$\bar{c}_f = \frac{0.0261}{\left(1 + 0.2M_\infty{}^2\right)^{0.418}\left(R_{\infty s}\right)^{1/7}}\left(\frac{T_\infty + 216}{T_t + 216}\right)^{1/7} \tag{9}$$

In these equations the Sutherland law of viscosity has been used to relate the viscosity at stagnation conditions to that at free-stream conditions. The equation for average flat-plate friction can be obtained from equation (9) by integrating $\bar{c}_f$ from 0 to l to yield

$$\bar{C}_F = \frac{0.0306}{\left(1 + 0.2M_\infty{}^2\right)^{0.418} R_{\infty,l}{}^{1/7}}\left(\frac{T_\infty + 216}{T_t + 216}\right)^{1/7} \tag{10}$$

The basic equation for this analysis (eq. (3)) was developed by using the incompressible average skin-friction law of Falkner and a compressibility correction based on an approximation to the method of reference 2 (see appendix A). This compressibility correction can be obtained by dividing equation (10) by the Falkner law, with the following result:

$$\frac{\bar{C}_F}{\bar{C}_{F,i}} = \frac{\left(\frac{T_\infty + 216}{T_t + 216}\right)^{1/7}}{\left(1 + 0.2M_\infty{}^2\right)^{0.418}} \tag{11}$$

A comparison of the results of equation (11) with the results of the Sommer and Short T' method of reference 2 is presented in figure 6. For the method of reference 2, the Kármán-Schoenherr incompressible friction law and a Reynolds number of 10×10^6 were used to obtain the compressibility factor. Figure 6 indicates that equation (11) provides a simple approximation to the Sommer and Short T' method of reference 2 with a fair degree of accuracy for the conditions of interest in the present analysis.

The results for turbulent flat-plate skin friction obtained by the Sommer and Short T' method of reference 2 are compared with the results of equation (10) in figure 7. The comparison indicates fair agreement between the methods for the conditions shown. However, skin friction obtained by the present method appears to vary much less with Reynolds number than does skin friction obtained by the Sommer and Short T' method. This difference is due to the basic difference between the Falkner law used in the present analysis and the Kármán-Schoenherr law used in the Sommer and Short T' method.

The basic equations of the present viscid analysis (eqs. (3) and (7)) can be reduced for the condition of conical flow by setting $\frac{q_e}{q_\infty} = \frac{M_e{}^2 p_e}{M_\infty{}^2 p_\infty}$, $r = Ks$, and $\frac{dM_e}{ds} = 0$. The

resulting expressions for the momentum thickness and local skin-friction coefficient on a cone are

$$\theta_c = \frac{0.00787 \exp\left(\Delta\eta/7R_g\right) M_\infty^{1/7} s^{6/7}}{\left[M_e R_\infty \left(1 + 0.2M_\infty^2\right)^{1.5}\right]^{1/7} \left(1 + 0.2M_e^2\right)^{0.204}} \left(\frac{T_\infty + 216}{T_t + 216}\right)^{1/7} \tag{12}$$

and

$$c_{f,c} = 0.0292 \exp\left(-\frac{6}{7}\frac{\Delta\eta}{R_g}\right)\left(\frac{M_e}{M_\infty}\right)^{13/7} \frac{\left(1 + 0.2M_\infty^2\right)^{3.286}}{\left(1 + 0.2M_e^2\right)^{3.704}} \left(\frac{T_\infty + 216}{T_t + 216}\frac{1}{R_\infty s}\right)^{1/7} \tag{13}$$

The local coefficient of equation (13) can be integrated over the surface of the cone and the resulting average friction coefficient can be written as follows:

$$C_{F,c} = 0.0315 \exp\left(-\frac{6}{7}\frac{\Delta\eta}{R_g}\right)\left(\frac{M_e}{M_\infty}\right)^{13/7} \frac{\left(1 + 0.2M_\infty^2\right)^{3.286}}{\left(1 + 0.2M_e^2\right)^{3.704}} \left(\frac{T_\infty + 216}{T_t + 216}\frac{1}{R_{\infty,l}}\right)^{1/7} \tag{14}$$

A comparison of these expressions with flat-plate expressions can be made by dividing equations (13) and (14) by the flat-plate expressions of equations (9) and (10), respectively. The results of this operation are

$$\frac{c_{f,c}}{\bar{c}_f} = 1.120 \exp\left(-\frac{6}{7}\frac{\Delta\eta}{R_g}\right)\left(\frac{M_e}{M_\infty}\right)^{13/7} \left(\frac{1 + 0.2M_\infty^2}{1 + 0.2M_e^2}\right)^{3.704} \tag{15}$$

and

$$\frac{C_{F,c}}{\bar{C}_F} = 1.035 \exp\left(-\frac{6}{7}\frac{\Delta\eta}{R_g}\right)\left(\frac{M_e}{M_\infty}\right)^{13/7} \left(\frac{1 + 0.2M_\infty^2}{1 + 0.2M_e^2}\right)^{3.704} \tag{16}$$

An examination of equations (15) and (16) indicates that, as the cones become slender, $M_e \to M_\infty$ and $\Delta\eta/R_g \to 0$ which reduces $c_{f,c}/\bar{c}_f$ and $C_{F,c}/\bar{C}_F$ to 1.120 and 1.035, respectively. Reference 10 gives representative values for these ratios to be 1.194 and 1.04, respectively, on the basis of the work of Van Driest and others.

VISCID-INVISCID INTERACTION

In the present analysis it is assumed that the viscid-inviscid interaction is sufficiently weak for the flows to be calculated separately, as outlined in the previous sections, and the interaction effects determined by iteration. The details of this technique can best be understood from an example problem. As a typical example, the calculation of the viscid and inviscid flow over an Adam's body with fineness ratio 10 and with a ratio of maximum area to base area of 1.88 is considered. Free-stream flow conditions are taken to be $M_\infty = 4.0$ and $R_{\infty,l} = 9.0 \times 10^6$. The variations of the important parameters of the first two iterations for the inviscid and viscid solutions are presented in figures 8(a) and 8(b), respectively. Initially, the inviscid analysis of the second-order shock-expansion method is applied to the body shape. In this example the body was represented by 70 elemental cone frustums. The resulting variations of C_p and M_e are shown in figure 8(a). With this initial inviscid solution assumed to provide conditions at the edge of the boundary layer, numerical solutions of the viscid equations can be provided and the results yield the boundary-layer growth and skin-friction coefficients shown in figure 8(b) for the first iteration. At this point a first-order mathematical model is available to describe the inviscid surface conditions and the boundary-layer growth.

The accepted method of evaluating the weak viscid-inviscid interaction is to calculate the inviscid solution for an effective body shape which is obtained by including the displacement thickness of the boundary layer. The boundary-layer growth is then reevaluated according to this effective-body inviscid solution. In the present analysis, the effective body shape is obtained from the displacement thickness as suggested in reference 14. The surface streamline displacement due to the presence of a boundary layer on a body of revolution in reference 14 is related to the displacement thickness of the present analysis by the following equation:

$$\delta^{**} = r\left(\sqrt{1 + 2\,\frac{\delta^*}{r}} - 1\right) \tag{17}$$

The effective body shape obtained for the second iteration of the example problem is shown in figure 8(a) along with the variations of C_p and M_e for this body shape. The effects of the viscid solution on the inviscid solution are indicated by the differences between the first and second iterations shown in figure 8(a). In order to obtain the effect of the change in the inviscid solution on the viscid solution, the results of figure 8(a) are used to reevaluate the boundary-layer growth and skin friction. The results of the reevaluation are shown as the second iteration in figure 8(b).

If the boundary layer is considered to be of finite thickness, then the inviscid conditions on the surface of the effective body do not represent those at the edge of the boundary layer. In the present analysis it is assumed that the Mach number on the surface of the effective body is propagated out to the edge of the boundary layer along a Mach line.

This assumption is represented schematically in figure 9. The geometry of figure 9 indicates that the Mach number distribution at the edge of the boundary layer can be approximated by the variation of the Mach number calculated for the surface of the effective body and transformed by the following relation:

$$\Delta x \approx (\delta - \delta^{**})\sqrt{M_{inv}^{2} - 1} \tag{18}$$

In equation (18) the value of δ is obtained from the previous iteration.

The Mach number distribution of figure 8(a) (second iteration) was transformed by equation (18) and used in the solution of the viscid equations to provide the second-iteration solution of the boundary-layer growth and the attendant skin friction. The comparison of the first- and second-iteration boundary-layer growth characteristics shown in figure 8(b) indicates little change. Further iteration did not yield significant changes in the solutions, and the second-iteration values of figure 8 are considered to be representative of the viscid-inviscid mathematical model of the flow including interations in the region of the body surface. The wave and friction components of the total drag can then be obtained by integration of the pressure and local friction coefficients over the body surface.

It has been mentioned previously that the solutions of the boundary-layer equations of the present analysis were numerical in nature and required the use of high-speed digital computers. Thus, the entire process described in the solution of the example problem has been programed for high-speed digital computation. A detailed description of the resulting computer program is presented in appendix B along with the necessary operating details. The program is designed to make as many iterations between the inviscid and viscid solutions as the user desires. For the remainder of the present analysis, all theoretical solutions, unless otherwise noted, will be the results of the second iteration obtained from the computer program presented in appendix B.

One difficulty which was encountered in the use of the present method involves the selection of the proper starting cone for the inviscid solution. This difficulty occurs when the shape of the body is such that a wide range of starting cones can be made tangent to the body surface in the region of the nose (i.e., a body with a rapid change of slope in the nose region). For bodies of this type it is recommended that the starting cone be

chosen such that the boundary layer is within the surface stream tube generated by the flow field of the starting cone. If this condition is satisfied, then for the expanding flow the entropy at the edge of the boundary layer remains constant and equal to the entropy of the flow field of the starting cone (an assumption of the second-order shock-expansion theory). An approximate criterion for the condition that the boundary layer be within the surface stream tube can be expressed as

$$y_a^2 > \left[(\delta + r)^2 - r^2\right] \tag{19}$$

where y_a is the radial coordinate of the conical shock point a in figure 1.

A criterion for the selection of the size of the body elements would be desirable. Unfortunately, no criterion is available to cover the wide range of body shapes and Mach numbers available to the user. It is suggested that the body be described by no less than 20 elements including the starting cone and, if the body shape is irregular (i.e., adverse and favorable gradients in combination), that this number of elements be increased until the surface pressures and skin friction show no significant change.

EVALUATION OF THE THEORETICAL METHOD

In this section the mathematical model which was developed in the previous section will be applied to several body shapes to describe the viscid and inviscid flow in the region of the body surface. The resulting viscid and inviscid drag estimates are compared with experimentally determined values where available. The viscid-inviscid interaction effects are accounted for herein by using the second-iteration values of the local surface conditions to determine the drag.

The body shape used in the first example is that of the NACA RM-10 missile body described in reference 10. The estimates of the momentum thickness and local skin-friction coefficients are shown in figure 10 along with the body shape. Figure 10 also includes some experimentally determined values of momentum thickness and local friction coefficients obtained from reference 10, and a comparison of the experiment and theory indicates good agreement of the present estimates.

Figure 11 compares the friction-drag and total-drag estimates of the present method with experimental values for the RM-10 missile body at several Mach numbers and Reynolds numbers. It should be noted that the experimental total-drag data of reference 10 were obtained by using the method of characteristics to provide the inviscid drag contribution and adding this directly to the friction drag which was obtained from velocity profile measurements. The experimental data from reference 15, however, were obtained by force and pressure measurement and are probably more accurate. A

comparison of the theory and experiment shown in figure 11 indicates that the present theoretical method is in good agreement with the experimental data from both references.

In order to examine boundary-layer behavior in the presence of strong favorable and adverse pressure gradients, reference 16 has provided experimental data on a low-fineness-ratio waisted body at several Mach numbers up to $M_\infty = 2.8$. The experimental values of the surface-pressure coefficients and local skin-friction coefficients are presented in figure 12 along with the body shape. The theoretical estimates of the surface pressures and skin friction are also shown in figure 12. It should be noted that these theoretical estimates were obtained with five iterations between the viscid and inviscid flow fields. The estimated surface pressures show good agreement with the experimental values of reference 16 except for $x/l > 0.7$, and the agreement of the skin-friction estimates and experimental values is fair. One obvious difficulty is the presence of a limited laminar run on the nose of the body (indicated by the lower values of the experimental data in the region of the nose). Although there is no inherent reason that the present technique cannot be extended to include a laminar run (the analysis of appendix A develops the growth of the momentum thickness including an initial laminar run), the present analysis does not account for this condition.

The surface pressures and local skin-friction data presented in reference 16 were integrated to give the friction and wave drag of the waisted body of revolution at the supersonic Mach numbers. The friction-drag and total-drag values are presented in figure 13 for a Reynolds number of 10×10^6. The theoretical estimates provided by the present method are indicated to be in good agreement with the experimental total drag.

The method of the present analysis was used to obtain theoretical estimates of the total drag of several body shapes over a wide range of flow conditions. The ratio of the theoretical drag coefficient predicted by the present method to the experimental drag coefficient is shown in figure 14 as a function of the hypersonic similarity parameter (see solid symbols). Also shown is the ratio of the theoretical to experimental drag coefficient, with the theoretical values obtained by using the supersonic area rule of reference 1 along with the flat-plate skin-friction method of reference 2 (see open symbols). The experimental values used were taken from references 10, 15, 16, and 17 and from present data obtained in the Langley Unitary Plan wind tunnel. It is significant to note that the supersonic-area-rule results are not reliable for conditions at $M_\infty/FR > 0.2$ whereas the present method gives reliable results at all conditions shown. In fact, all the cases considered in figure 14 indicate the present method to be within 10 percent of the reported experimental drag values, with all except four points being within 5 percent. In view of the difficulties associated with obtaining accurate experimental drag data (i.e., attaining fully turbulent flow, measuring base pressure, etc.), it is believed that the present method is generally as accurate as the current experimental testing techniques.

CONCLUDING REMARKS

An approximate mathematical model of the inviscid and viscid flow field about a body of revolution has been developed by utilizing modifications of the second-order shock-expansion theory and of a theoretical analysis of compressible boundary-layer growth with pressure gradient. The area of application of this model is intended to be restricted to the attached bow-shock condition in the supersonic flow regime with an all-turbulent boundary layer. The viscid-inviscid interaction is accounted for by iteration between the respective theories. The solution of the mathematical model including the iteration and the integration of surface conditions to give wave and friction drags has been programed for digital computation, and the program is included.

The inviscid solution is shown to compare well with the method of characteristics for a wide range of body shapes including local surface compressions and moderate amounts of boattail. The basic theory has been extended to provide an estimate of the flow-field pressures and shock shape.

The viscid solution in its simplified flat-plate and conical forms is demonstrated to agree well with the established flat-plate and cone solutions for a turbulent boundary layer. The theoretical estimates of the local skin friction were in good agreement with experimental values for a body with moderate pressure gradient; even for a condition of strong favorable and adverse gradient on the same body, fair agreement was indicated.

The viscid and inviscid solutions including interactions were applied to several body shapes over a wide range of test conditions, and the resulting total drag estimates generally agreed with the reported experimental values to within 5 percent. In view of the difficulty involved in obtaining precise experimental data, it is believed that the present method is generally as accurate as the current experimental testing techniques.

Langley Research Center,
National Aeronautics and Space Administration,
Langley Station, Hampton, Va., December 6, 1968,
722-01-00-02-23.

APPENDIX A

MODIFICATION OF EXISTING EXPRESSION FOR MOMENTUM THICKNESS

The analysis of reference 5 develops an equation which describes the momentum thickness on a body of revolution with pressure gradient in compressible flow. The approach taken in reference 5 is to transform the incompressible equation of reference 8 by means of the transformations described in reference 9. The present development of the momentum-thickness expression follows the approach of reference 5 with these two modifications:

(1) The reference temperature equation of reference 2 is used.

(2) The viscosity is assumed to vary as the square root of the temperature.

The starting point for the present development is taken to be the incompressible momentum-thickness equation of reference 8 which is expressed as (in the notation of the present paper)

$$\theta_i = \frac{1}{u_{e,i}^3 R}\left\{\left[f_{lam}\nu_t \int_0^{S_T} u_{e,i}^5 R^2 dS\right]^{7/12} + f_{turb}\nu_t^{1/6} \int_{S_T}^{S} u_{e,i}^{10/3} R^{7/6} dS\right\}^{6/7} \tag{A1}$$

The transformation of this equation to the compressible form is accomplished according to reference 5 by the following equations:

$$\left.\begin{aligned} dS &= \left(\frac{a_e}{a_t}\right)^{\frac{3\gamma-1}{\gamma-1}} ds \\ dY' &= \frac{a_e}{a_t}\frac{\rho}{\rho_t} dy' \\ u_i &= \frac{a_t}{a_e} u \\ u_{e,i} &= \frac{a_t}{a_e} u_e \\ R &= r \end{aligned}\right\} \tag{A2}$$

In the process of this transformation, reference 5 and the present analysis make the assumptions that there is no heat transfer, that the pressure is constant through the

boundary layer in the direction normal to the body surface, that the Prandtl number is unity, and that the flow external to the boundary layer is isentropic.

The left-hand side of equation (A1) can be conveniently transformed by equations (A2) if, for purposes of this transformation only, the boundary layer is assumed to be small with respect to the body radius so that the momentum thickness can be expressed as

$$\theta = \int_0^{\delta} \frac{\rho u}{\rho_e u_e}\left(1 - \frac{u}{u_e}\right)dy' \tag{A3}$$

With the assumption indicated in equation (A3) and the transformations of equations (A2), the incompressible momentum thickness is related to the compressible value by

$$\theta_i = \left(\frac{a_e}{a_t}\right)^{\frac{\gamma+1}{\gamma-1}} \theta \tag{A4}$$

Most of the terms on the right-hand side of equation (A1) can be directly transformed by equations (A2). However, the transformation of the f terms is complicated by the fact that according to reference 5 they are related to the average flat-plate friction coefficients by

$$f = \left(\frac{u_{e,i} l_i}{\nu_t}\right)^n \left(\frac{\overline{C_{F,i}}}{2}\right)^{1+n} \tag{A5}$$

The value of n is 1 for laminar conditions and 1/6 for turbulent conditions.

In order to transform the f terms, it is first necessary to establish the transformation for the average flat-plate friction. Reference 5 shows that if the Blasius equation is used for the laminar average friction relation, the transformed value of f_{lam} does not differ from the incompressible value which is determined to be 0.441. The value of f_{turb} on the other hand is shown to be 0.0076 for the incompressible case when the Falkner relation is used for $\overline{C_{F,i}}$, and the transformation to the compressible case involves the reference temperature concept. The present analysis follows the transformation of reference 5 with a modified reference temperature relation and a modified viscosity-temperature relation. The reference temperature equation of the present analysis is that of reference 2 for adiabatic wall conditions and is given as

$$\frac{T^*}{T_e} = 1 + 0.1142 M_e^2 = \left(\frac{a^*}{a_e}\right)^2 \tag{A6}$$

The viscosity-temperature relation of the present analysis is

$$\frac{\mu_e}{\mu_t} = \sqrt{\frac{T_e}{T_t}} = \frac{a_e}{a_t} \tag{A7}$$

The average flat-plate incompressible skin-friction coefficient obtained from the Falkner equation can be transformed by equations (A2), (A6), and (A7) to provide the expression for the compressible skin-friction coefficient as follows:

$$\overline{C_{F,turb}} = \left(\frac{a_e}{a_t}\right)^{3/7}\left(\frac{a_e}{a^*}\right)^{11/7} \frac{0.0306}{\left(\frac{\rho_t u_i \ell_i}{\mu_t}\right)^{1/7}} \tag{A8}$$

The curve fit of figure 15 shows that equation (A8) can be further simplified without significant loss of accuracy in the $0 \leqq M_e \leqq 5.0$ range by replacing a_e/a^* with $\left(\frac{a_e}{a_t}\right)^{5/7}$. With this simplification and equations (A2) and (A5), the results of equation (A8) can be combined to provide the desired transformed coefficient f_{turb}. The value of f_{turb} can be simply expressed as

$$f_{turb} = 0.0076\left(\frac{a_t}{a_e}\right)^{11/21} \tag{A9}$$

With the results of equations (A2), (A4), and (A9), the incompressible momentum-thickness expression of equation (A1) can be transformed to the compressible form with the following result:

$$\theta = \frac{\left(1 + \frac{\gamma - 1}{2} M_e^2\right)^3}{M_e^3 r}\left\{\left[0.441 \frac{\nu_t}{a_t}\int_0^{s_T} \frac{M_e^5 r^2 ds}{\left(1 + \frac{\gamma - 1}{2} M_e^2\right)^4}\right]^{7/12} + \frac{0.0076\left(\frac{\nu_t}{a_t}\right)^{1/6}}{\left(1 + \frac{\gamma - 1}{2} M_e^2\right)^{-11/42}} \int_{s_T}^{s} \frac{M_e^{10/3} r^{7/6} ds}{\left(1 + \frac{\gamma - 1}{2} M_e^2\right)^4}\right\}^{6/7} \tag{A10}$$

For the condition of an all-turbulent boundary layer, equation (A10) becomes

$$\theta = \frac{\left(1 + 0.2M_e^2\right)^3}{M_e^3 r}\left[\frac{0.0076\left(\frac{\nu_t}{a_t}\right)^{1/6}}{\left(1 + 0.2M_e^2\right)^{-11/42}} \int_0^{s} \frac{M_e^{10/3} r^{7/6} ds}{\left(1 + 0.2M_e^2\right)^4}\right]^{6/7} \tag{A11}$$

APPENDIX B

COMPUTER PROGRAM TO OBTAIN VISCID AND INVISCID DRAG CONTRIBUTIONS FOR A BODY OF REVOLUTION

A process is discussed in the text for obtaining the inviscid solution of the flow field and the solution of a mathematical model of the boundary-layer growth on a body of revolution. This process includes the numerical solution of the viscid and inviscid equations as well as an iteration between the two solutions to provide interaction effects. The numerical solution and iteration have been programed for high-speed digital computation, and the program includes an integration of the local surface pressures and skin friction to provide the respective drag contributions. The purpose of this appendix is to provide a description of the necessary input and available output as well as a FORTRAN listing of the source program with an example input case and the resulting output listing.

Description of Program

The program reads the body geometry in terms of x,y coordinates which are used to represent the elemental conical frustums of the body in the numerical process. The starting cone is generated by extending the slope of the first elemental frustum forward to provide the full cone. The inviscid solution is then calculated for the midpoints of the frustum elements. Numerical derivatives are taken from linear interpolation of the inviscid quantities, and the viscid equations are solved.

The boundary-layer growth is then used to provide an effective body shape for the second iteration. The program continues iterating between the viscid and inviscid solutions for a specified number of iterations. The inviscid flow fields and the resulting boundary-layer growth are output for each iteration along with the wave and friction drags. For convenience the flat-plate friction drag is output along with the values for the body of revolution.

Program Listing

The FORTRAN listing of the source program used at the Langley Research Center on the Control Data 6600 computer system is presented as follows:

```
      PROGRAM VBODY(INPUT,OUTPUT,TAPE5=INPUT,TAPE6=OUTPUT)
      DIMENSION WHAT(10), X(200), Y(200), XANS(200), PANS(200), AMANS(20
     10), CP(200), XS(200), YS(200), DEL(200), ANGLE(200), PC(200), A(4)
     2, TEMP(8), ROOT(3), DLSOR(13,11), DELTAT(13,11), PCT(13,11), AM1T(
     313,11), THET1T(13,11), MTAB(11), CDWS(200), XT(200), CFT(200), CFT
     42(200), MT2(200), DLSTAR(200), YSAVE(200), THODLT(200), V(200), DE
     5LTT(200), XTT(200), XL(200), XOL(200), YOL(200), THETAT(200)
      COMMON XANS,AMANS,MT2,DLSTAR,N,XT,S,CFT,CFT2,V,DELSOR,AM,RN,THODLT
     1,X,I,DELTT,Y,O,YSAVE,PANS,DEL,T,CDWS,XL,THETAT,XTT,ANGLE,CP,XOL,YO
     2L,YMAX,ITER,ICODE,ST(200)
      COMPLEX TEMP,ROOT
      REAL MIDDLE,MT2,MTAB
      NAMELIST /NUM/ DELTAT,AM,PCT,AM1T,THET1T,N,X,Y,MT2,DLSOR,RN,THODLT
     1,O,MTAB,ITER,TO
1     READ (5,29) WHAT
      READ (5,NUM)
      ICODE=1
      T=TO/(1.+AM**2/5.)
      DO 2 I=1,N
      XOL(I)=X(I)/X(N)
      DELTT(I)=0.
      DLSTAR(I)=0.
      YOL(I)=Y(I)/X(N)
2     YSAVE(I)=Y(I)
      YMAX=YSAVE(1)
      DO 3 I=2,N
3     YMAX=AMAX1(YMAX,YSAVE(I))
      ST(1)=SQRT(X(1)**2+Y(1)**2)
      DO 4 I=2,N
4     ST(I)=SQRT((Y(I)-Y(I-1))**2+(X(I)-X(I-1))**2)+ST(I-1)
      S=3.1416*YMAX**2/144.
5     WRITE (6,33) WHAT
      WRITE (6,35) ICODE,AM,RN
      WRITE (6,37)
      DEL(1)=57.295779*ATAN((Y(2)-Y(1))/(X(2)-X(1)))
      DO 6 I=2,N
6     DEL(I)=57.295779*ATAN((Y(I)-Y(I-1))/(X(I)-X(I-1)))
      WRITE (6,38) (X(I),Y(I),DEL(I),I=1,N)
      DEL(1)=ATAN((Y(2)-Y(1))/(X(2)-X(1)))
      CALL BILUP (DELTAT,MTAB,PCT,AM1T,THET1T,DLSOR,13,11,DEL(1),AM,PC(1
     11),AMANS(1),THETA1,DELSOR)
      THETA=THETA1*57.29577
      WRITE (6,36) AMANS(1),THETA,DELSOR
      XANS(1)=X(1)/2.
      PANS(1)=PC(1)
      CP(1)=(PANS(1)-1.)/(AM**2*.7)
      AMU=ATAN((1./AMANS(1))/SQRT(1.-(1./AMANS(1))**2))+DEL(1)
      YS(1)=(Y(1)-(Y(1)/TAN(DEL(1)))*SIN(AMU)/COS(AMU))/(1.-SIN(AMU)/COS
     1(AMU)/SIN(THETA1)*COS(THETA1))
      XS(1)=YS(1)/SIN(THETA1)*COS(THETA1)-Y(1)/TAN(DEL(1))+X(1)
      CDWS(1)=CP(1)*(YSAVE(1)**2)*3.1416
      AMA=AMANS(1)
      ANGLE(1)=(DEL(1)+ASIN(1./AMA))*57.29577
      DPDSA=0
      PA=PC(1)
      WRITE (6,39)
      WRITE (6,40) XANS(1),PANS(1),AMANS(1),CP(1),XS(1),YS(1),ANGLE(1),C
     1DWS(1)
```

```
      DO 25 I=2,N
      DEL(I)=ATAN((Y(I)-Y(I-1))/(X(I)-X(I-1)))
      IF (DEL(I).LT.0.) GO TO 7
      DELTA=DEL(I)
      CALL BILUP (DELTAT,MTAB,PCT,PCT,PCT,PCT,13,11,DEL(I),AM,PC(I),PC(I
     1),PC(I),PC(I))
      GO TO 8
7     PC(I)=1.
8     ANUA=2.4495*ATAN(.40825*SQRT(AMA**2-1.))-ATAN(SQRT(AMA**2-1.))
      ANUB=ANUA+DEL(I-1)-DEL(I)
      IF (ANUB.GE.ANUA) GO TO 14
      IF (ABS(DEL(I-1)-DEL(I)).LT..00001) GO TO 14
C
C     CALCULATION FOR COMPRESSION AND SHOCK FORMATION
C
      ANG=DEL(I)-DEL(I-1)
      A(1)=1.0
      A(2)=-(AMA**2+2.)/AMA**2-1.4*SIN(ANG)**2
      A(3)=(2.*AMA**2+1.)/AMA**4+(2.4**2/4.+.4/AMA**2)*SIN(ANG)**2
      A(4)=-COS(ANG)**2/AMA**4
      CALL FALG (A,3,0,ROOT,TEMP,IERR)
      AR1=REAL(ROOT(1))
      AI1=AIMAG(ROOT(1))
      AR2=REAL(ROOT(2))
      AI2=AIMAG(ROOT(2))
      AR3=REAL(ROOT(3))
      AI3=AIMAG(ROOT(3))
      IF (IERR) 9,10,9
9     WRITE (6,30) ROOT
      GO TO 27
C
C     TEST TO FIND IMAGINARY ROOTS
C
10    IF (ABS(AI1).LT..00001.AND.ABS(AI2).LT..00001.AND.ABS(AI3).LT..000
     101) GO TO 11
      WRITE (6,31) A(2),A(3),A(4),ROOT
      GO TO 27
C
C     CHECK FOR MIDDLE ROOT
C
11    BIG=AMAX1(AR1,AR2,AR3)
      SMALL=AMIN1(AR1,AR2,AR3)
      DO 12 J=1,3
      IF (REAL(ROOT(J)).LT.BIG.AND.REAL(ROOT(J)).GT.SMALL) GO TO 13
12    CONTINUE
      WRITE (6,32) ROOT
      IF (I.NE.2) GO TO 22
      PB=PA
      AMB=AMA
      GO TO 22
13    MIDDLE=SQRT(REAL(ROOT(J)))
      SIGMA=ASIN(MIDDLE)
      SINSQ=SIN(SIGMA)**2
      AMB=SQRT((36.*AMA**4*SINSQ-5.*(AMA**2*SINSQ-1.)*(7.*AMA**2*SINSQ+5
     1.))/((7.*AMA**2*SINSQ-1.)*(AMA**2*SINSQ+5.)))
      PB=(7.*AMA**2*SINSQ-1.)/6.*PA
      AMUB=SIN(1./AMB)
      XX=(2.4*TAN(DEL(I)-DEL(I-1))*COS(SIGMA-DEL(I-1))-SIN(SIGMA-DEL(I-1
```

```
     1)))*AMA**2*SIN(SIGMA-DEL(I-1))**2+SIN(SIGMA-DEL(I-1))
      YY=1.+(1.-2.*SIN(SIGMA-DEL(I-1))**2+2.*TAN(DEL(I)-DEL(I-1))*SIN(SI
     1GMA-DEL(I-1))*COS(SIGMA-DEL(I-1)))*AMA**2*SIN(SIGMA-DEL(I-1))**2
      F=4./2.4*(1.+.4/2.*AMA**2)*SIN(SIGMA-DEL(I-1))*XX/YY
      BA=1.4*PA*AMA**2/(2.*(AMA**2-1.))
      BB=1.4*PB*AMB**2/(2.*(AMB**2-1.))
      XY=2.*BB/(Y(I)-1.)*(SIN(SIGMA-DEL(I-1))*SIN(DEL(I-1))/SIN(SIGMA-DE
     1L(I))-SIN(DEL(I)))+DPDSA*(BB*SIN(SIGMA-DEL(I-1))/(BA*SIN(SIGMA-DEL
     2(I)))+(PB/PA-F)*COS(SIGMA-DEL(I-1))*TAN(AMUB)/SIN(SIGMA-DEL(I)))
      DPDS=XY/(1.+TAN(AMUB)/TAN(SIGMA-DEL(I)))
      GO TO 21
14    DELM=.01
      K=1
      AMB=AMA
15    AMB=AMB+DELM
      ANU=2.4495*ATAN(.40825*SQRT(AMB**2-1.))-ATAN(SQRT(AMB**2-1.))
      IF (ANU-ANUB) 15,15,16
16    AMB=AMB-DELM
      GO TO (17,18,19,20), K
17    DELM=.001
      K=2
      GO TO 15
18    DELM=.0001
      K=3
      GO TO 15
19    DELM=.00001
      K=4
      GO TO 15
20    PB=PA*((1.+AMA**2/5.)/(1.+AMB**2/5.))**3.5
      BA=1.4*PA*AMA**2/(2.*(AMA**2-1.))
      AOASTA=((125./216.)/AMA)*(1.+AMA**2/5.)**3
      BB=1.4*PB*AMB**2/(2.*(AMB**2-1.))
      AOASTB=((125./216.)/AMB)*(1.+AMB**2/5.)**3
      DPDS=(BB/Y(I-1))*(AOASTA/AOASTB*SIN(DEL(I-1))-SIN(DEL(I)))+BB/BA*A
     1OASTA/AOASTB*DPDSA
21    ETA=DPDS*(X(I)-X(I-1))/((PC(I)-PB)*COS(DEL(I)))
      IF (ETA) 22,23,23
22    WRITE (6,34)
      PANS(I)=PB
      AMANS(I)=AMB
      AMA=AMB
      PA=PB
      XANS(I)=(X(I)+X(I-1))/2.
      DPDSA=0.
      GO TO 24
23    PA=PC(I)-(PC(I)-PB)*EXP(-ETA)
      AMA=SQRT(5.*((1.+AMB**2/5.)*(PB/PA)**.28571-1.))
      XANS(I)=(X(I)+X(I-1))/2.
      ETANS=ETA/2.
      PANS(I)=PC(I)-(PC(I)-PB)*EXP(-ETANS)
      AMANS(I)=SQRT(5.*((1.+AMB**2/5.)*(PB/PANS(I))**.28571-1.))
      DPDSA=(PC(I)-PA)/(PC(I)-PB)*DPDS
24    CP(I)=(PANS(I)-1.)/(AM**2*.7)
      CDWS(I)=CDWS(I-1)+CP(I)*(YSAVE(I)**2-YSAVE(I-1)**2)*3.1416
      AMU=ATAN((1./AMANS(I))/SQRT(1.-(1./AMANS(I))**2))+DEL(I)
     C=SQRT((6.*PANS(I)+1.)/(7.*AM**2))
     THETA=ATAN(C/SQRT(1.-C**2))
     YS(I)=(Y(I)+(XS(I-1)-X(I))*SIN(AMU)/COS(AMU)-SIN(AMU)/COS(AMU)*COS
```

```
     1(THETA)/SIN(THETA)*YS(I-1))/(1.-SIN(AMU)/COS(AMU)*COS(THETA)/SIN(T
     2HETA))
      ANGLE(I)=(DEL(I)+ASIN(1./AMANS(I)))*57.29577
      XS(I)=XS(I-1)+(YS(I)-YS(I-1))/SIN(THETA)*COS(THETA)
25    WRITE (6,40) XANS(I),PANS(I),AMANS(I),CP(I),XS(I),YS(I),ANGLE(I),C
     1DWS(I)
      CALL BOUND
      ICODE=ICODE+1
      IF (ICODE.GT.ITER) GO TO 27
      I=N
      DO 26 KK=1,I
      XNEW=X(KK)/12.
      CALL FTLUP (XNEW,DLSTNW,+1,I,XT,DLSTAR)
      DLSTNW=DLSTNW*12.
      Y(KK)=YSAVE(KK)*SQRT(1.+2.*DLSTNW/YSAVE(KK))
      XOL(KK)=X(KK)/X(N)
26    YOL(KK)=Y(KK)/X(N)
      GO TO 5
27    DO 28 I=1,N
28    Y(I)=YSAVE(I)
      GO TO 1
C
29    FORMAT (12A6)
30    FORMAT (15H  ERROR IN FALG/2X,6E17.8)
31    FORMAT (17H  IMAGINARY ROOTS,3E17.8/6E17.8)
32    FORMAT (17H  TWO EQUAL ROOTS/2X,6E17.8)
33    FORMAT (1H1,///1X,12A6)
34    FORMAT (1X25HIST ORDER SHOCK EXPANSION)
35    FORMAT (///32X14HINPUT      DATA,10X,12HITERATION   I2///37X2HM=F5.
     12/36X3HRN=E15.8//)
36    FORMAT (12X19HSTARTING CONE -  M=F8.5,4X6HTHETA=F8.3,4X7HDELSOR=F8
     1.4///)
37    FORMAT (24X1HX,14X1HY,13X5HDELTA//)
38    FORMAT (20XF8.4,7XF8.4,7XF8.4)
39    FORMAT (////36X6HOUTPUT//15X17HINVISCID SOLUTION//11X4HX,IN,5X8HP/
     1P(INF),5X1HM,10X2HCP,6X7HX-SHOCK,5X7HY-SHOCK,1X20HCHARACTERISTIC A
     2NGLE,2X9HD/Q,SQ IN)
40    FORMAT (7X,F8.4,3X,F9.5,3X,F7.4,3X,F7.4,2X,F10.4,2X,F10.4,8X,F8.4,
     16X,F10.6)
      END



      SUBROUTINE BOUND
      DIMENSION THETAT(200), DTHODX(200), DMODX(200), CFT(200), SUM(4),
     1FOFX(4), THET2(200), CFT2(200), DTHDX2(200), XT(200), DYODX(200),
     2THODLT(200), X(200), YSAVE(200), PANS(200), XANS(200), AMANS(200),
     3 MT2(200), DLSTAR(200), Y(200), V(200), DELTT(200), DEL(200), CDWS
     4(200), XTT(200), ANGLE(200), XL(200)
      COMMON XANS,AMANS,MT2,DLSTAR,N,XT,S,CFT,CFT2,V,DELSOR,AM,RN,THODLT
     1,X,I,DELTT,Y,O,YSAVE,PANS,DEL,T,CDWS,XL,THETAT,XTT,ANGLE,CP(200),X
     2OL(200),YOL(200),YMAX,ITER,ICODE,ST(200)
      REAL MT,MT2,NUTOAT,MP1,MM1,M,NUTAT2
      EXTERNAL FUNC
      XT(1)=XANS(1)/12.
      CFT2(1)=0.
      CFT(1)=0.
      XTT(1)=0.
      V(1)=YSAVE(1)/24.
```

```
      DO 1 I=2,N
      XT(I)=XANS(I)/12.
      CFT2(I)=0.
      CFT(I)=0.
      XTT(I)=XT(I)+(DELTT(I)-DLSTAR(I))*SQRT(AMANS(I)**2-1.)
      IF (XTT(I).GT.XTT(I-1)) GO TO 1
      XTT(I)=XTT(I-1)+X(N)/12000.
1     V(I)=(YSAVE(I)+YSAVE(I-1))/24.
      NUTAT2=AM*(1.+AM**2/5.)**(-2.5)/RN*(1.+216./T)/(1.+216./T/(1.+AM**
     12/5.))
      NUTOAT=NUTAT2*EXP(DELSOR)
      DO 2 I=1,N
      XL(I)=XT(I)/X(N)*12.
      A1=0.
      CALL FTLUP (XANS(I),SS,+1,N,X,ST)
      B1=SS/12.
      CALL MGAUSS (A1,B1,15,SUM,FUNC,FOFX,4)
      THET2(I)=(1.+.4/2.*AM**2)**(-.2)*(.0076*NUTAT2**(.167)*(SS/12.))**
     1(.857)/(AM**(.145))
      CALL FTLUP (XT(I),AMANX,+1,N,XTT,AMANS)
2     THETAT(I)=(1.+.4/2.*AMANX**2)**3/(AMANX**3*V(I))*(.0076*NUTOAT**.1
     167/((1.+.4/2.*AMANX**2)**(-.262))*SUM(1))**.857
      DO 3 I=1,N
      XP1=XT(I)+.001
      XM1=XT(I)-.001
      CALL FTLUP (XP1,THETP1,+1,N,XT,THETAT)
      CALL FTLUP (XM1,THETM1,+1,N,XT,THETAT)
      CALL FTLUP (XP1,MP1,+1,N,XTT,AMANS)
      CALL FTLUP (XM1,MM1,+1,N,XTT,AMANS)
      CALL FTLUP (XP1,THETP2,+1,N,XT,THET2)
      CALL FTLUP (XM1,THETM2,+1,N,XT,THET2)
      CALL FTLUP (XP1,YP1,+1,N,XT,V)
      CALL FTLUP (XM1,YM1,+1,N,XT,V)
      XD=XT(I)*12.
      CALL FTLUP (XD,DL,+1,N,X,DEL)
      DYDDX(I)=(YP1-YM1)/(XP1-XM1)*COS(DL)
      DTHDDX(I)=(THETP1-THETM1)/(XP1-XM1)*COS(DL)
      DTHDX2(I)=(THETP2-THETM2)/(XP1-XM1)*COS(DL)
3     DMODX(I)=(MP1-MM1)/(XP1-XM1)*COS(DL)
      DMODX(1)=DMODX(3)
      DMODX(2)=DMODX(3)
      DO 10 I=1,N
      CALL FTLUP (XT(I),M,+1,N,XTT,AMANS)
      CALL FTLUP (XT(I),THETT,+1,N,XT,THETAT)
      A=1./(1.+.2*M**2)
      B=1.-A
      NSUM1=(O-1.)/2.
      SUM1=0.
      DO 4 II=1,NSUM1
4     SUM1=SUM1+(B**II/(2.*FLOAT(II)**2+FLOAT(II)))
      NSUM2=O-1.
      SUM2=1.
      DO 5 II=1,NSUM2
5     SUM2=SUM2+(B**II/((FLOAT(II)+1.)*(2.*FLOAT(II)+1.)))
      CALL FTLUP (M,THODL,+1,51,MT2,THODLT)
6     DELTT(I)=1./THODL*THETAT(I)
      DELOR=DELTT(I)/V(I)
      CTHODL=O/2.*A/B**((O+1.)/2.)*(2.-ALOG(A)+1./SQRT(B)*ALOG((1.-SQRT(
```

```
     1B))/(1.+SQRT(B)))-SUM1)+DELOR*O/2.*A/B**O*(1./B*ALOG(A)-1./SQRT(B)
     2*ALOG((1.-SQRT(B))/(1.+SQRT(B)))-SUM2)
      IF ((1.-(THODL/CTHODL)).LT..001) GO TO 7
      THODL=CTHODL
      GO TO 6
7     SUM3=0.
      DO 8 II=1,NSUM1
8     SUM3=SUM3+B**II/FLOAT(II)
      SUM4=1.
      DO 9 II=1,NSUM2
9     SUM4=SUM4+B**II/(2.*FLOAT(II)+1.)
      DSTODL=1.+1./2.*DELOR+O/2.*A/(B**((O+1.)/2.))*(SUM3+ALOG(A))+DELOR
     1*O*A/B**O*(SUM4-1./(2.*SQRT(B))*ALOG((1.+SQRT(B))/(1.-SQRT(B))))
      DELSTR=DSTODL/CTHODL
      DLSTAR(I)=DELSTR*THETT
      CFT2(I)=2.*DTHDX2(I)
10    CFT(I)=((DTHODX(I)+THETT*(1./V(I)*DYODX(I)+(2.-M**2+DELSTR)/(M*(1.
     1+.4/2.*M**2))*DMODX(I)))*2.)*(M/AM)**2*PANS(I)
      A1=0.
      B1=X(N)/12.
      CALL MGAUSS (A1,B1,15,SUM,FUNC,FOFX,4)
      CFFIN=SUM(2)/SUM(4)
      CFFIN2=SUM(3)/SUM(4)
      CDW=CDWS(N)/S/144.
      CDFR=SUM(2)/S
      CDTOT=CDW+CDFR
      WRITE (6,11) (XL(I),THETAT(I),CFT(I),CFT2(I),DLSTAR(I),DELTT(I),I=
     11,N)
      WRITE (6,12) CFFIN,CFFIN2
      WRITE (6,13) CDW,CDFR,CDTOT
      RETURN
C
11    FORMAT (/21X16HVISCOUS SOLUTION//16X3HX/L,7X8HTHETA,FT3X46HBODY-CF
     1,LOCAL FLAT PLATE CF,LOCAL  DEL STAR,FT4X8HDELTA,FT/(F21.5,F13.8,F
     214.8,2F17.8,F14.8))
12    FORMAT (/24X14HBODY-CF,TOTAL=F11.8,7X20HFLAT-PLATE CF,TOTAL=F11.8)
13    FORMAT (/18X8HCD,WAVE=F11.8,7X12HCD,FRICTION=F11.8,7X9HCD,TOTAL=F1
     11.8)
      END



      SUBROUTINE FUNC (XX,FOFX)
      DIMENSION XANS(200), AMANS(200), MT2(200), DLSTAR(200), XT(200), C
     1FT(200), CFT2(200), V(200), PANS(200), FOFX(4), Y(200), YSAVE(200)
     2, THODLT(200), X(200), DELTT(200), DEL(200), CDWS(200), XTT(200),
     3ANGLE(200), XL(200), THETAT(200)
      COMMON XANS,AMANS,MT2,DLSTAR,N,XT,S,CFT,CFT2,V,DELSOR,AM,RN,THODLT
     1,X,I,DELTT,Y,O,YSAVE,PANS,DEL,T,CDWS,XL,THETAT,XTT,ANGLE,CP(200),X
     20L(200),YOL(200),YMAX,ITER,ICODE,ST(200)
      REAL MM
      CALL FTLUP (XX,YVAL,+1,N,XT,V)
      IF (YVAL.LT.O) YVAL=O.
      CALL FTLUP (XX,MM,+1,N,XT,AMANS)
      CALL FTLUP (XX,CF,+1,N,XT,CFT)
      XD=XX*12.
```

```
      CALL FTLUP (XD,DL,+1,N,X,DEL)
      FOFX(1)=(MM**3.33*YVAL**1.167/((1.+.4/2.*MM**2)**4))/COS(DL)
      FOFX(2)=2.*3.1416*YVAL*CF
      CALL FTLUP (XX,CF2,+1,N,XT,CFT2)
      FOFX(3)=2.*3.1416*YVAL*CF2
      FOFX(4)=2.*3.1416*YVAL
      RETURN
      END


      SUBROUTINE BILUP (TABI,TABJ,TABIJ,TACIJ,TADIJ,TAEIJ,NI,NJ,VALI,VAL
     1J,BVAL1,CVAL1,DVAL1,EVAL1)
C     A TWO DIMENSIONAL TABLE LOOK-UP FOR TWO VARIABLES.
C     INPUT TABLES ARE TABIJ(I,J),TACIJ(I,J),TADIJ(I,J) AND TAEIJ(I,J)
C     AS FUNCTIONS OF TABI(I) AND TABJ(J). THE TWO DEPENDENT VARIABLES A
C     LINEARLY INTERPOLATED SIMULTANEOUSLY FOR INPUT VALUES OF VALI AND
C     VALJ RESULTING IN ANSWERS BVAL1, CVAL1, DVAL1, EVAL1.  ERROR
C     SIGNALS ARE GENERATED WHEN THE TABJ(J) TABLE IS EXTRAPOLATED.
      DIMENSION TABJ(11), TABI(13,11), TABIJ(13,11), TACIJ(13,11), TADIJ
     1(13,11), TAEIJ(13,11), TBISL(2), TBIJ1(2), TCIJ1(2), TDIJ1(2), TEI
     2J1(2)
      TBJSL=0.0
      KK=2
      IF (TABJ(1).LT.TABJ(2)) GO TO 4
      DO 2 J=1,NJ
      IF (VALJ-TABJ(J)) 2,1,3
1     TBJSL=1.0
      GO TO 8
2     CONTINUE
      IF (J.EQ.NJ) WRITE (6,22)
3     IF (J.GT.1) GO TO 8
      WRITE (6,23)
      J=2
      GO TO 8
4     DO 6 J=1,NJ
      IF (VALJ-TABJ(J)) 7,5,6
5     TBJSL=1.0
      GO TO 8
6     CONTINUE
      IF (J.EQ.NJ) WRITE (6,22)
7     IF (J.GT.1) GO TO 8
      WRITE (6,23)
      J=2
8     IF (TABI(1,J).GT.TABI(2,J)) GO TO 12
      IF (VALI.LT.TABI(1,J)) GO TO 10
      IF (VALI.GT.TABI(NI,J)) GO TO 11
      DO 9 I=1,NI
      IF (VALI-TABI(I,J)) 17,16,9
9     CONTINUE
10    I=2
      GO TO 17
11    I=NI
      GO TO 17
12    IF (VALI.GT.TABI(1,J)) GO TO 14
      IF (VALI.LT.TABI(NI,J)) GO TO 15
      DO 13 I=1,NI
      IF (VALI-TABI(I,J)) 13,16,17
13    CONTINUE
```

```
14      I=2
        GO TO 17
15      I=NI
        GO TO 17
16      TBISL(KK)=0.0
        TBIJ1(KK)=TABIJ(I,J)
        TCIJ1(KK)=TACIJ(I,J)
        TDIJ1(KK)=TADIJ(I,J)
        TEIJ1(KK)=TAEIJ(I,J)
        GO TO 18
17      TBISL(KK)=(VALI-TABI(I-1,J))/(TABI(I,J)-TABI(I-1,J))
        TBIJ1(KK)=TBISL(KK)*(TABIJ(I,J)-TABIJ(I-1,J))+TABIJ(I-1,J)
        TCIJ1(KK)=TBISL(KK)*(TACIJ(I,J)-TACIJ(I-1,J))+TACIJ(I-1,J)
        TDIJ1(KK)=TBISL(KK)*(TADIJ(I,J)-TADIJ(I-1,J))+TADIJ(I-1,J)
        TEIJ1(KK)=TBISL(KK)*(TAEIJ(I,J)-TAEIJ(I-1,J))+TAEIJ(I-1,J)
18      IF (TBJSL.EQ.0.0) GO TO 19
        BVAL1=TBIJ1(KK)
        CVAL1=TCIJ1(KK)
        DVAL1=TDIJ1(KK)
        EVAL1=TEIJ1(KK)
        GO TO 21
19      IF (KK.EQ.1) GO TO 20
        KK=KK-1
        J=J-1
        GO TO 8
20      J=J+1
        TBJSL=(VALJ-TABJ(J-1))/(TABJ(J)-TABJ(J-1))
        BVAL1=TBJSL*(TBIJ1(2)-TBIJ1(1))+TBIJ1(1)
        CVAL1=TBJSL*(TCIJ1(2)-TCIJ1(1))+TCIJ1(1)
        DVAL1=TBJSL*(TDIJ1(2)-TDIJ1(1))+TDIJ1(1)
        EVAL1=TBJSL*(TEIJ1(2)-TEIJ1(1))+TEIJ1(1)
21      RETURN
C
22      FORMAT (/20X20HHIGH J EXTRAPOLATION)
23      FORMAT (/20X19HLOW J EXTRAPOLATION)
        END


        SUBROUTINE MGAUSS (A,B,N,SUM,FUNC,FOFX,NUMBER)
C            THIS SUBROUTINE INTEGRATES FROM ZERO TO ONE
        DIMENSION U(5), R(5), SUM(1), FOFX(1)
        DO 1 LL=1,NUMBER
1       SUM(LL)=0.0
        IF (A.EQ.B) RETURN
        U(1)=.4255628305091 84
        U(2)=.2833023029353 76
        U(3)=.1602952158504 88
        U(4)=.0674683166555 08
        U(5)=.0130467357414 14
        R(1)=.1477621123573 76
        R(2)=.1346333596549 98
        R(3)=.1095431812579 91
        R(4)=.0747256745752 90
        R(5)=.0333567215434 4
        FINE=N
        DELTA=FINE/(B-A)
```

```
      DO 3 K=1,N
      XI=K-1
      FINE=A+XI/DELTA
      DO 2 II=1,5
      UU=U(II)/DELTA+FINE
      CALL FUNC (UU,FOFX)
      DO 2 JOYBOY=1,NUMBER
2     SUM(JOYBOY)=R(II)*FOFX(JOYBOY)+SUM(JOYBOY)
      DO 3 JJ=1,5
      UU=(1.0-U(JJ))/DELTA+FINE
      CALL FUNC (UU,FOFX)
      DO 3 NN=1,NUMBER
3     SUM(NN)=R(JJ)*FOFX(NN)+SUM(NN)
      DO 4 IJK=1,NUMBER
4     SUM(IJK)=SUM(IJK)/DELTA
      RETURN
      END


      SUBROUTINE FALG (COEFFS,N,I,ROOT,TEMP,IERR)
      DIMENSION COEFFS(1), TEMP(1), ROOT(1)
      DIMENSION XIDIFF(2), RDIFF(2), APPROX(3)
      COMPLEX F,FPR,APPROX,TEMP,ROOT
      COMPLEX TEMPM
      COMPLEX RELTST
      NSAVE=N
      IERR=0
      IB=0
      ICLEAN=2*N+2
C           CLEAR WORKING AREA
      DO 1 LLL=1,ICLEAN
1     TEMP(LLL)=0.0
C           CLEAR ROOT STORAGE
      DO 2 LLL=1,N
2     ROOT(LLL)=0.0
C           CONSTANTS TO TEST
C           CONVERGENCE
      CONST=.1E-6
C           OVERFLOW
      OVCON=1.E150
C           MAGNITUDE OF ROOTS
      RCONST=1.E-21
C           JONJON=0,FIRST ITERATION
      JONJON=0
C           CHECK CONSTANT TERM FOR ZERO
      JJJ=1
      NCO=N+1
3     IF (I.NE.1) GO TO 4
C           COMPLEX COEFFICIENTS
      NCO=2*NCO
      IF (COEFFS(NCO-1).NE.0.) GO TO 5
C           HERE IF REAL COEFFICIENTS
4     IF (COEFFS(NCO).NE.0.) GO TO 5
C           ROOT=ZERO
      ROOT(JJJ)=0.
      NCO=NCO-1
      JJJ=JJJ+1
```

```
C           REDUCE DEGREE AND IF 1,STORE ROOT AND EXIT
      N=N-1
      IF (N.NE.1) GO TO 3
      ROOT(JJJ)=0.
      GO TO 38
C
C           ENTRY  FIRST AND SECOND ITERATIONS
5     J=JJJ
      NTERMS=N+1
      KCONJ=0
C           CLEAR APPROX
      APPROX(1)=0.0
      APPROX(2)=0.0
      APPROX(3)=0.0
      IF (I.EQ.1) GO TO 7
C           REAL COEFFICIENTS
      DO 6 IJFF=1,NTERMS
6     TEMP(IJFF)=CMPLX(COEFFS(IJFF),0.0)
      GO TO 9
C           COMPLEX COEFFICIENTS
7     DO 8 IIIX=1,NTERMS
8     TEMP(IIIX)=CMPLX(COEFFS(2*IIIX-1),COEFFS(2*IIIX))
C
C           CHECK LEADING COEFFICIENT FOR 0 OR 1
9     TEMPL=REAL(TEMP(1))
      IF (TEMPL.NE.0.) GO TO 10
C           IF REAL IS ZERO,CHECK IMAGINARY
      TEMPL=AIMAG(TEMP(1))
      IF (TEMPL.NE.0.) GO TO 10
C           LEADING COEFFICIENT ZERO                IERR=1
      IERR=1
      GO TO 38
C           DIVIDE BY LEADING COEFFICIENT
10    TEMPM=TEMP(1)
      DO 11 LLA=1,NTERMS
11    TEMP(LLA)=TEMP(LLA)/TEMPM
C           KCONJ=1, TRIAL VALUE=CONJUGATE
C
12    IF (KCONJ.NE.0) GO TO 13
C           FIRST TRIAL VALUE
      APPROX(1)=(.01,.01)
C     DIFFERENTIATE
13    DO 14 II=1,NTERMS
      XPON=NTERMS-II
      NNOW=II+NTERMS
14    TEMP(NNOW)=XPON*TEMP(II)
      NPON=NTERMS-1
C           KA=0 FOR FIRST TRIAL VALUE
      KA=0
C
C           JONJON=1     SECOND ITERATION
15    IF (JONJON.EQ.1) APPROX(1)=ROOT(J)
C           CLEAR RDIFF,XIDIFF
      DO 16 LLL=1,2
      RDIFF(LLL)=0.0
16    XIDIFF(LLL)=0.0
C
C           ROOT EVALUATION
```

```
C           MAXIMUM ITERATIONS =120
17      L=2
        PARTR1=REAL(APPROX(1))
        PARTM1=AIMAG(APPROX(1))
        DO 25 K=2,121
C           EVALUATE F(X)
18      F=(0.0,0.0)
        DO 19 II=1,NTERMS
        F=APPROX(L-1)*F+TEMP(II)
        XF=ABS(REAL(F))
        YF=ABS(AIMAG(F))
C           CHECK FOR OVERFLOW
        IF (XF.GT.OVCON.OR.YF.GT.OVCON) GO TO 26
19      CONTINUE
C           EVALUATE FPRIME(X)
        FPR=(0.0,0.0)
        DO 20 JJ=1,NPON
        NNOW=JJ+NTERMS
        FPR=APPROX(L-1)*FPR+TEMP(NNOW)
        YFP=ABS(AIMAG(FPR))
        XFP=ABS(REAL(FPR))
C           CHECK FOR OVERFLOW
        IF (XFP.GT.OVCON.OR.YFP.GT.OVCON) GO TO 26
20      CONTINUE
C           SEE IF FPRIME=0
        IF (XFP.EQ.0.0.AND.YFP.EQ.0.0) GO TO 26
C           IF NOT ZERO,NEW APPROXIMATION
        APPROX(L)=APPROX(L-1)-F/FPR
        PARTR2=REAL(APPROX(L))
        PARTM2=AIMAG(APPROX(L))
C           SET EITHER PART TO ZERO IF LESS THAN 1.E-21
        IF (ABS(PARTR2).LE.RCONST) PARTR2=0.
        IF (ABS(PARTM2).LE.RCONST) PARTM2=0.
        IF (PARTR2.EQ.0..AND.PARTM2.EQ.0.) GO TO 21
        GO TO 22
C           ZERO ROOT
21      IF (L.EQ.3) APPROX(2)=APPROX(3)
        GO TO 30
C
22      RDIFF(L-1)=ABS(PARTR2-PARTR1)
        XIDIFF(L-1)=ABS(PARTM2-PARTM1)
        IF (L.EQ.3) GO TO 23
        L=3
        PARTR1=PARTR2
        PARTM1=PARTM2
        GO TO 18
C
C           TEST 1
23      IF ((RDIFF(2)+XIDIFF(2)).LT.(RDIFF(1)+XIDIFF(1))) GO TO 24
C           TEST 2
        RELTST=(APPROX(3)-APPROX(2))/APPROX(3)
        DIFFR=ABS(REAL(RELTST))
        DIFFXI=ABS(AIMAG(RELTST))
        IF (DIFFR.LT.CONST.AND.DIFFXI.LT.CONST) GO TO 30
24      APPROX(2)=CMPLX(PARTR2,PARTM2)
        PARTR1=PARTR2
        PARTM1=PARTM2
        RDIFF(1)=RDIFF(2)
25      XIDIFF(1)=XIDIFF(2)
```

```
C
C           MAXIMUM ITERATIONS EXCEEDED OR
C           OVERFLOW OR
C           FPRIME=0
C           TRY AGAIN WITH SECOND TRIAL VALUE
26      IF (JONJON.EQ.1) GO TO 27
        IF (KA.EQ.105) GO TO 28
        APPROX(1)=(1.,1.)
        KA=105
        GO TO 17
C           SECOND ITERATION  NONCONVERGENT ROOT  IERR=3
27      IERR=3
C           STORE RESULT AND IMPROVE NEXT ROOT
        GO TO 34
C
C           FIRST ITERATION  ROOT R NONCONVERGENT   IERR=2
C           IMPROVE (R-1) ROOTS
28      IERR=2
C           IB=LAST CONVERGENT ROOT
        IB=J
        ROOT(J)=APPROX(2)
        IF (IB.NE.1) GO TO 29
C           FIRST ROOT FAILED     RETURN
        GO TO 38
29      JONJON=1
        GO TO 5
C
C           STORE ROOTS
30      IF (JONJON.EQ.1) GO TO 34
C           HERE IF FIRST ITERATION
        ROOT(J)=APPROX(2)
C           REDUCE POLYNOMIAL BY SYNTHETIC DIVISION
        NTERMS=NTERMS-1
        DO 31 IK=2,NTERMS
        TEMP(IK)=ROOT(J)*TEMP(IK-1)+TEMP(IK)
31      CONTINUE
C           NEXT ROOT IF COMPLEX COEFFICIENTS
        IF (I.EQ.1) GO TO 33
C           HERE IF REAL COEFFICIENTS
        IF (KCONJ.EQ.0) GO TO 32
C           RESET KCONJ IF ROOT IS CONJUGATE OF PREVIOUS ROOT
        KCONJ=0
        GO TO 33
32      X=REAL(ROOT(J))
        Y=AIMAG(ROOT(J))
        IF (X.EQ.0.) GO TO 33
C           SEE IF REAL OR COMPLEX
        IF (ABS(Y/X).LE.1.E-10) GO TO 33
C           COMPLEX ROOT      TRIAL VALUE=CONJUGATE
        APPROX(1)=CONJG(ROOT(J))
        KCONJ=1
C           NEXT ROOT
33      J=J+1
        IF (J.NE.NSAVE) GO TO 12
C           LAST ROOT
        ROOT(J)=-TEMP(2)/TEMP(1)
        JONJON=1
        GO TO 5
```

```
C
C           IMPROVED ROOT FROM SECOND ITERATION
34      ROOT(J)=APPROX(2)
        X=ABS(REAL(ROOT(J)))
        Y=ABS(AIMAG(ROOT(J)))
C           SET REAL OR IMAG. TO ZERO IF LESS THAN RCONST
        IF (X.LT.RCONST.AND.Y.LT.RCONST) GO TO 35
        IF (X.LT.RCONST) ROOT(J)=CMPLX(0.0,AIMAG(ROOT(J)))
        IF (Y.LT.RCONST) ROOT(J)=CMPLX(REAL(ROOT(J)),0.0)
        GO TO 37
35      IF (X.GE.Y) GO TO 36
        ROOT(J)=CMPLX(0.0,AIMAG(ROOT(J)))
        GO TO 37
36      ROOT(J)=CMPLX(REAL(ROOT(J)),0.0)
C
C           IF(R-1) ROOTS IMPROVED,RETURN
37      IF (J.EQ.IB) GO TO 38
        J=J+1
C           IF N ROOTS IMPROVED,RETURN
        IF (J.LE.NSAVE) GO TO 15
38      N=NSAVE
        RETURN
        END


        SUBROUTINE FILUP (X,Y,M,N,VARI,VARD)
        DIMENSION VARI(1), VARD(1), V(3), YY(2)
        IF (M.EQ.0.AND.N.EQ.0) GO TO 19
        IF (M.EQ.0.AND.N.NE.0) GO TO 21
        IF (N.LE.IABS(M)) GO TO 21
        IF (M.GT.0) GO TO 8
C               M.LT.0
        DO 1 IYY=1,N
        I=IYY
        IF (VARI(I)-X) 2,20,1
1       CONTINUE
        I=N+M
C           IF X.LT.X(N),EXTRAPOLATE
        IF (M.EQ.-1) GO TO 3
        GO TO 7
C           IF X.GT.X(1),EXTRAPOLATE
2       IF (I.EQ.1.AND.M.EQ.-1) GO TO 3
        IF (I.EQ.1.AND.M.EQ.-2) GO TO 7
        IF (M.NE.-1) GO TO 4
C           M=-1
        I=I-1
3       IF (VARI(I).LE.VARI(I+1)) GO TO 21
        GO TO 12
C           M=-2
4       IF (I.NE.N) GO TO 5
        I=N-2
        GO TO 7
C           COMPARE WITH NEXT
5       IF (VARI(I+1)-X) 6,21,21
6       I=I-1
        IF (I.EQ.1) GO TO 7
C           SEE WHICH THREE
        IF ((VARI(I-1)-X).LT.(X-VARI(I+2))) I=I-1
7       IF (VARI(I).LE.VARI(I+1).OR.VARI(I+1).LE.VARI(I+2)) GO TO 21
        GO TO 17
```

APPENDIX B – Continued

```
C              M.GT.0
8      DO 9 IYY=1,N
       I=IYY
       IF (X-VARI(I)) 10,20,9
9      CONTINUE
       I=N-M
C           IF X.GT.X(N),EXTRAPOLATE
       IF (M.EQ.1) GO TO 11
       GO TO 16
C           IF X.LT.X(1),EXTRAPOLATE
10     IF (I.EQ.1.AND.M.EQ.1) GO TO 11
       IF (I.EQ.1.AND.M.EQ.2) GO TO 16
       IF (M.NE.1) GO TO 13
C           M=I
       I=I-1
11     IF (VARI(I+1).LE.VARI(I)) GO TO 21
C           LINEAR
12     Y=(VARD(I)*(VARI(I+1)-X)-VARD(I+1)*(VARI(I)-X))/(VARI(I+1)-VARI(I)
      1)
       RETURN
C           M=2
13     IF (I.NE.N) GO TO 14
       I=N-2
       GO TO 16
C           COMPARE WITH NEXT
14     IF (X-VARI(I+1)) 15,21,21
15     I=I-1
       IF (I.EQ.1) GO TO 16
C           SEE WHICH THREE
       IF ((X-VARI(I-1)).LT.(VARI(I+2)-X)) I=I-1
16     IF (VARI(I+1).LE.VARI(I).OR.VARI(I+2).LE.VARI(I+1)) GO TO 21
C           SECOND ORDER
17     V(1)=VARI(I)-X
       V(2)=VARI(I+1)-X
       V(3)=VARI(I+2)-X
       K=I
       DO 18 J=1,2
       YY(J)=(VARD(K)*V(J+1)-VARD(K+1)*V(J))/(VARI(K+1)-VARI(K))
18     K=K+1
       Y=(YY(1)*V(3)-YY(2)*V(1))/(VARI(I+2)-VARI(I))
       RETURN
C              ZERO ORDER(Y=Y(1))
19     Y=VARD(1)
       RETURN
C              Y=Y(1)
20     Y=VARD(I)
       RETURN
C
C           ERROR PRINT
21     PRINT 22
       PRINT 23, M,N,X
       IF (N.EQ.0) STOP
       IF (M.EQ.0) STOP
       PRINT 24
       STOP
C
22     FORMAT (/31H ERROR WAS ENCOUNTERED IN FTLUP)
23     FORMAT (1X,2HM=I5,5X,2HN=I5,5X,2HX=E20.8)
24     FORMAT (19H TABLE OUT OF ORDER)
       END
```

Description of Input Data

A single case consists of the determination of the inviscid flow field, body surface conditions, and boundary-layer growth along a meridian line from the nose to the base of the body of revolution. The Mach number, unit Reynolds number, and free-stream stagnation temperature must be put into the program in order to define the free-stream flow conditions. It is necessary to use as input, in addition to the body geometry, a table of cone surface pressures, cone surface Mach numbers, cone shock angles, and cone entropy changes for a range of Mach numbers and cone half-angles. In addition, a table of the two-dimensional values of θ/δ for a range of Mach numbers is required for the desired velocity profile index. The number of iterations to be made between the viscid and inviscid solutions must also be specified. For the loading routine used in the program, any column except the first may be used on the input cards unless otherwise specified, and a decimal format is used for the input quantities unless a fixed point number is specified. The FORTRAN names and a description of the required inputs are as follows:

FORTRAN	Available card columns	Description
WHAT	1 to 72	Identification card (any identifying information may be written on this card and will appear at the start of output for each case)
$NUM	2 to 5	Arbitrary name required by the loading routine to define the block of input data
AM	2 to 80	Free-stream Mach number
RN	2 to 80	Unit Reynold's number, 12/model units
N	2 to 80	Number of body coordinates specified (Fixed point number; 200 points maximum)
X(1)	2 to 80	Body x-coordinate array, model units
Y(1)	2 to 80	Body y-coordinate array, model units
TO	2 to 80	Stagnation temperature, ^{o}R
O	2 to 80	Velocity profile index
MT2(1)	2 to 80	Mach number array for two-dimensional boundary-layer parameter θ/δ (51 points)
THODLT(1)	2 to 80	θ/δ array (51 points)

FORTRAN	Available card columns	Description
MTAB(1)	2 to 80	Mach number array for cone tables (11 points)
DELTAT(1,1)	2 to 80	Cone half-angle array for cone tables (two-dimensional array; 13 points columnwise, 11 points rowwise), radians
PCT(1,1)	2 to 80	Cone surface pressure p_c/p_∞ (two-dimensional array; 13 points columnwise, 11 points rowwise)
AMIT(1,1)	2 to 80	Cone surface Mach number (two-dimensional array; 13 points columnwise, 11 points rowwise)
THET1T(1,1)	2 to 80	Cone shock angle (two-dimensional array; 13 points columnwise, 11 points rowwise), radians
DLSOR(1,1)	2 to 80	Entropy change across the cone shock, $\Delta\eta/R_g$ (two-dimensional array; 13 points columnwise, 11 points rowwise)
ITER	2 to 80	Number of iterations to be made between viscid and inviscid solutions (fixed point number)
$	2	Denotes the end of a case

The system loading subroutine used in the program (NAMELIST) is quite flexible in that the order of the input cards is unimportant and successive cases can be run by repeating the WHAT and $NUM cards followed by only the changed parameters and a $ card.

Example Input Listing

As an example of a set of input cards, the following is a listing of the inputs necessary to compute the viscid and inviscid flow parameters on the RM-10 body at $M_\infty = 2.2$ and $R_\infty = 4.16 \times 10^6$ with two iterations specified:

```
RM 10 BODY
$NUM
 MTAB(1)=1.5,2.,2.5,3.,3.5,4.,4.5,5.,6.,8.,10.,
   DELTAT(1,1)=0.,.04363323,.08726645,.13089967,.1745329,.2181661,.2617993,
          .3054325,.3490658,.392699,.4363322,.479965,.5235987,
            0.,.04363323,.08726645,.13089967,.1745329,.2181661,.2617993,
          .3054325,.3490658,.392699,.4363322,.479965,.5235987,
            0.,.04363323,.08726645,.13089967,.1745329,.2181661,.2617993,
          .3054325,.3490658,.392699,.4363322,.479965,.5235987,
            0.,.04363323,.08726645,.13089967,.1745329,.2181661,.2617993,
          .3054325,.3490658,.392699,.4363322,.479965,.5235987,
            0.,.04363323,.08726645,.13089967,.1745329,.2181661,.2617993,
          .3054325,.3490658,.392699,.4363322,.479965,.5235987,
            0.,.04363323,.08726645,.13089967,.1745329,.2181661,.2617993,
          .3054325,.3490658,.392699,.4363322,.479965,.5235987,
            0.,.04363323,.08726645,.13089967,.1745329,.2181661,.2617993,
          .3054325,.3490658,.392699,.4363322,.479965,.5235987,
            0.,.04363323,.08726645,.13089967,.1745329,.2181661,.2617993,
          .3054325,.3490658,.392699,.4363322,.479965,.5235987,
            0.,.04363323,.08726645,.13089967,.1745329,.2181661,.2617993,
          .3054325,.3490658,.392699,.4363322,.479965,.5235987,
            0.,.04363323,.08726645,.13089967,.1745329,.2181661,.2617993,
          .3054325,.3490658,.392699,.4363322,.479965,.5235987,
            0.,.04363323,.08726645,.13089967,.1745329,.2181661,.2617993,
          .3054325,.3490658,.392699,.4363322,.479965,.5235987,
 PCT(1,1)=1.,1.0194326,1.0624668,1.1218836,1.1949823,1.2805338,1.3780493,
          1.4875334,1.6094921,1.7452173,1.8977323,1.,1.,
      1.,1.0302014,1.095048,1.1836274,1.2924832,1.4202392,1.5662549,
          1.73013,1.9114873,2.1099574,2.325245,2.5572482,2.8063347,
      1.,1.0430054,1.1338127,1.2579479,1.4118223,1.5943908,1.8051501,
          2.0435503,2.3088209,2.5999833,2.9158958,3.2553311,3.6170774,
      1.,1.0575531,1.1779135,1.3434709,1.5510936,1.8002508,2.0905385,
          2.4211572,2.7908532,3.1979721,3.6405103,4.1162105,4.6226939,
      1.,1.07368,1.2270211,1.4399168,1.7101605,2.0377458,2.4222429,
          2.8624798,3.3565651,3.9019948,4.4957647,5.1344738,5.8144615,
      1.,1.0912720,1.2809867,1.547292,1.8892065,2.3071757,2.8006264,
          3.3678429,4.0061275,4.7119593,5.4811532,6.3089994,7.1904022,
      1.,1.1102609,1.3397531,1.6656866,2.0884875,2.6089172,3.2261054,
          3.9376627,4.7398834,5.6280810,6.5967119,7.6395491,8.7499419,
      1.,1.1305848,1.403315,1.7952468,2.308246,2.9432816,3.6990542,
          4.5722872,5.558163,6.6506071,7.8425504,9.1261264,10.492909,
      1.,1.1750571,1.5449088,2.0883718,2.8100784,3.7110158,4.7885278,
          6.0371455,7.4492676,9.0156074,10.725597,12.5675,14.528819,
      1.,1.2786974,1.8871344,2.8137638,4.0675451,5.6477433,7.5471315,
          9.7541022,12.253764,15.028693,18.059352,21.32435,24.8000936,
  1.,1.4015141,2.3102668,3.7291669,5.6691937,8.1254669,11.084206,
  14.525483,18.425183,22.755513,27.485425,32.581175,38.00706,
```

```
AM1T(1,1)=1.5,1.4866884,1.4579318,1.4197316,1.3748579,1.3248992,1.2707392,
          1.2127162,1.1506488,1.0837313,1.0100703,1.,1.,
        2.,1.9808615,1.9415254,1.8912335,1.8340453,1.7721933,1.7068837,
          1.6386764,1.5677572,1.4940884,1.417468,1.3375202,1.2535953,
      2.5,2.4729472,2.4193976,2.3528628,2.2788768,2.2001554,2.1179422,
          2.0327606,1.9448503,1.8543543,1.7613748,1.6659616,1.5680718,
        3.,2.96276,2.8913832,2.8048038,2.7101402,2.6103929,2.5067511,
          2.3997895,2.2899646,2.1777409,2.063583,1.9479054,1.8310067,
      3.5,3.4500939,3.3571597,3.2467499,3.1275136,3.0025569,2.8731152,
          2.7400668,2.6043443,2.466913,2.3286833,2.1904152,2.0526629 ,
        4.,3.93477,3.8164543,3.6783916,3.530568,3.3761469,3.2166972,
          3.0537628,2.8889908,2.7239783,2.5600783,2.3983186,2.2393739,
      4.5,4.4166246,4.269058,4.0994611,3.9189007,3.730775,3.5374323,
          3.3414321,3.1453333,2.9513677,2.7612386,2.5760876,2.3965344,
        5.,4.8955305,4.7148078,4.5097079,4.2921847,4.0662668,3.8355932,
          3.6040616,3.3752078,3.1517935,2.935687,2.7279347,2.5289133,
        6.,5.8440686,5.5852474,5.2968787,4.9927832,4.6801702,4.3668118,
          4.0597311,3.7640785,3.4829712,3.2178167,2.9687934,2.735258,
        8.,7.7018785,7.2390804,6.7337145,6.2103924,5.6922672,5.198150,
          4.7389543,4.3187765,3.9373126,3.5918831,3.2787858,2.9940481,
    10.,9.50464,8.7725147,7.9851813,7.197758,6.456834,5.7867581,5.1933727,
    4.6723717,4.2153623,3.8131019,3.4569163,3.139194,
THET1T(1,1)=.72979225,.72979225,.73078309,.73489674,.74466072,.76158205,
.78592365,.81737375,.85571959,.90132794,.95578504,1.,1.,
   .5236989,.5236989,.52524879,.53140177,.54464827,.56518145,.5919218,
          .62370115,.65966167,.69928055,.74232301,.78882392,.83913453,
.41168587,.41168587,.41425491,.42357796,.44136238,.46630615,.496626,
          .53101645,.56864312,.60899456,.6517773,.6968639,.74427222,
.34011057,.34011057,.34409993,.35701069,.37899374,.40760084,.44085123,
          .47752193,.51687237,.55844619,.60196673,.64728576,.69436247,
.29017134,.29017134,.29591943,.31238763,.33790128,.36939419,.40494077,
          .44344094,.48423753,.52692147,.57123978,.61704946,.66429713,
.25329402,.25329402,.26104195,.28078488,.3091822,.34295689,.3803207,
          .42028295,.46225228,.5058584,.55087169,.5971618,.64467684,
.22495268,.22495268,.2348371,.25747371,.28822452,.32383435,.36266044,
          .40380119,.44671754,.49107302,.53666064,.5833645,.63114,
   .2025178,.2025178,.21458047,.23972546,.27241579,.30952796,.34954864 ,
          .39164866,.43533264,.48029511,.52635069,.57339789,.62140105,
.16936998,.16936998,.18564567,.21481181,.2504916,.28990367,.33173775,
          .37527812,.42010459,.46596496,.51271277,.56027373,.60862959,
.12931031,.12931031,.15261801,.18711985,.22663938,.26894684,.31300625,
          .35827161,.40443925,.45133986,.49888523,.54704135,.59581671,
    .10660326,.10660326,.13498608,.17279866,.21462672,.25860856,.30390795,
   .35010593,.39698293,.44442555,.49238318,.54084699,.58984179,
```

```
 DLSOR(1,1)=0.,0.,0.,.0000002,.00000573,.00005236,.00026419,.00090125,
         .0023587,.00514317,.00989938,.00989938,.00989938,
        0.,0.,0.,.0000031,.00005746,.00040704,.00162363,.00452431,.00996314,
  .01866783,.03116991,.04781193,.06880882,
         0.,0.,.00000028,.00002575,.00035647,.00195845,.00640297,
 .01530889,.02991039,.05091317,.07853234,.11260453,.15271789,
        0.,0.,.00000218,.00013394,.00140073,.00623076,.0174901,.0373587,
  .06695116,.10642165,.15522653,.21239054,.27672371,
  0.,0.,.00001098,.00048559,.00397466,.01496156,.03739172,.07337245,
         .12323764,.18607002,.26023292,.34376991,.43467831,
           0.,0.,.00004119,.00134715,.0089929,.02966745,.06773287,
    .12442398,.19867459,.28812978,.38990179,.50105232,.6188581,
  0.,.00000012,.00012344,.0030712,.01732983,.0514303,.10922787,
         .19030359,.29173079,.4095372,.53959966,.67812008,.82183021,
   0.,.0000002,.0003097,.00605144,.02971067,.08086374,.161855550,.26996484,
          .4001399,.54678565,.70468605,.86938119,1.0372605,
   0.,.00000185,.00131425,.01730657,.06852806,.16323286,.29803005,
   .46440851,.65298408,.85541135,1.0649734,1.2765648,1.486461,
   0.,.00003844,.00889343,.06884447,.20612165,.41208982,.66585564,
   .94742268,1.2414942,1.5375068,1.8285879,2.1104825,2.3807193,
   0.,.00030054,.02981173,.16533512,.41495684,.74144435,1.1072541,1.4860364,
   1.8616789,2.2251066,2.5716249,2.8991281,3.2070205,
MT2(1)=0.,.2,.4,.6,.8,1.,1.2,1.4,1.6,1.8,2.,2.2,2.4,2.6,2.8,3.,3.2,3.4,3.6,
3.8,4.,4.2,4.4,4.6,4.8,5.,5.2,5.4,5.6,5.8,6.,6.2,6.4,6.6,6.8,7.,7.2,7.4,
7.6,7.8,8.,8.2,8.4,8.6,8.8,9.,9.2,9.4,9.6,9.8,10.,
O=7.,
THODLT(1)=1.,.09695,.09616,.09487,.09315,.09104,.08862,.08595,
.08311,.08016,.07714,.0741,.07108,.06812,.06522,.0624,
.05969,.05708,.05458,.05219,.04992,.04775,.0457,
.04374,.04189,.04013,.03846,.03688,.03539,.03397,
.03262,.03135,.03014,.02899,.0279,.02686,.02588,.02495,
.02406,.02321,.02241,.02164,.02091,.02021,.01955,.01891,
.01831,.01773,.01717,.01665,.01614,
 ITER=2,
TO=570.,
N=52,
X(1)=.25,.5,1.,2.,3.,4.,5.,6.,7.,8.,9.,10.,11.,12.,13.,14.,15.,16.,17.,18.,19.,
20.,21.,22.,23.,24.,25.,26.,27.,28.,29.,30.,31.,32.,33.,34.,35.,36.,37.,38.,
39.,40.,41.,42.,43.,44.,45.,46.,47.,48.,49.,50.,
 Y(1)=.0331,.066,.1308,.2573,.3795,.4973,.6107,.7199,.8247,.9251,1.0212,1.113,
 1.2004,1.2835,1.3623,1.4367,1.5067,1.5725,1.6339,1.6909,1.7436,1.792,1.836,
 1.8757,1.9111,1.9421,1.9687,1.9911,2.0091,2.0227,2.032,2.037,2.0376,2.0339,
 2.0259,2.0135,1.9967,1.9757,1.9503,1.9205,1.8864,1.848,1.8052,1.7581,1.7067,
 1.6509,1.5907,1.5263,1.4575,1.3843,1.3068,1.225,
RN=4.17E06,
AM=2.2,
$
```

It should be noted that the input tables of conical flow parameters were obtained from reference 7 and need not be changed from case to case unless better coverage is desired. Similarly the input tables of θ/δ were obtained from reference 13 for a velocity-profile-index value of 7 and need not be changed unless better coverage is desired or the user wishes to examine the results for a value of the velocity profile index other than 7. Only odd values of the velocity profile index can be used in the program.

Description of Output Data

The output format of the program is arranged so that each iteration of a single case contains a listing of body coordinates, free-stream conditions, starting cone conditions, longitudinal variation of the inviscid parameters, shock coordinates, characteristic angles, longitudinal variations of the viscid parameters including flat-plate friction coefficients, integrated total-friction coefficients (body of revolution and flat-plate values) based on body surface area, and wave-drag, friction-drag, and total-drag coefficients based on body maximum cross-sectional area. It should be noted that the body coordinates presented for the second and succeeding iterations are the coordinates of the effective body and are used only in the solution of the inviscid parameters. The units shown in the output listing are correct only when the body coordinates are in inches.

Example Output Listing

The following is an example output listing for the RM-10 body at the conditions specified by the example input case previously presented:

RM 10 BODY

INPUT DATA ITERATION 1

M= 2.20
RN= 4.17000000E+06

X	Y	DELTA
.2500	.0331	7.4219
1.0000	.1308	7.4219
2.0000	.2573	7.2096
3.0000	.3795	6.9670
4.0000	.4973	6.7185
5.0000	.6107	6.4697
6.0000	.7199	6.2320
7.0000	.8247	5.9828
8.0000	.9251	5.7333
9.0000	1.0212	5.4893
10.0000	1.1130	5.2451
11.0000	1.2004	4.9950
12.0000	1.2835	4.7504
13.0000	1.3623	4.5056
14.0000	1.4367	4.2550
15.0000	1.5067	4.0042
16.0000	1.5725	3.7646
17.0000	1.6339	3.5135
18.0000	1.6909	3.2623
19.0000	1.7436	3.0167
20.0000	1.7920	2.7710
21.0000	1.8360	2.5194
22.0000	1.8757	2.2734
23.0000	1.9111	2.0274
24.0000	1.9421	1.7756
25.0000	1.9687	1.5237
26.0000	1.9911	1.2832
27.0000	2.0091	1.0312
28.0000	2.0227	.7792
29.0000	2.0320	.5328
30.0000	2.0370	.2865
31.0000	2.0376	.0344
32.0000	2.0339	-.2120
33.0000	2.0259	-.4584
34.0000	2.0135	-.7104
35.0000	1.9967	-.9625
36.0000	1.9757	-1.2030
37.0000	1.9503	-1.4550
38.0000	1.9205	-1.7069
39.0000	1.8864	-1.9530
40.0000	1.8480	-2.1991
41.0000	1.8052	-2.4508
42.0000	1.7581	-2.6966
43.0000	1.7067	-2.9424
44.0000	1.6509	-3.1938
45.0000	1.5907	-3.4450
46.0000	1.5263	-3.6848
47.0000	1.4575	-3.9357
48.0000	1.3843	-4.1866
49.0000	1.3068	-4.4316
50.0000	1.2250	-4.6764

STARTING CONE – M= 2.07766 THETA= 27.963 DELSOR= .0000

OUTPUT

INVISCID SOLUTION

X,IN	P/P(INF)	M	CP	X-SHOCK	Y-SHOCK	CHARACTERISTIC ANGLE	D/Q,SQ IN
.1250	1.21015	2.0777	.0620	.7569	.4040	36.1930	.000213
1ST ORDER SHOCK EXPANSION							
.6250	1.21015	2.0777	.0620	3.5098	1.9672	36.1930	.003334
1.5000	1.20054	2.0828	.0592	7.3956	4.1636	35.9036	.012463
2.5000	1.18891	2.0890	.0558	11.5841	6.5177	35.5675	.026095
3.5000	1.17743	2.0952	.0524	16.1037	9.0438	35.2263	.043088
4.5000	1.16613	2.1014	.0490	20.9907	11.7602	34.8862	.062444
5.5000	1.15557	2.1072	.0459	26.2378	14.6616	34.5628	.083405
6.5000	1.14430	2.1135	.0426	32.0112	17.8363	34.2220	.105064
7.5000	1.13318	2.1197	.0393	38.3270	21.2900	33.8818	.126760
8.5000	1.12248	2.1258	.0362	45.2099	25.0338	33.5503	.148002
9.5000	1.11181	2.1319	.0330	52.7965	29.1381	33.2186	.168315
10.5000	1.10084	2.1382	.0298	61.2908	33.7080	32.8783	.187222
11.5000	1.09039	2.1443	.0267	70.6541	38.7186	32.5475	.204521
12.5000	1.08031	2.1503	.0237	81.1047	44.2823	32.2194	.220048
13.5000	1.07029	2.1562	.0207	93.0007	50.5827	31.8856	.233621
14.5000	1.06067	2.1620	.0179	106.4822	57.6874	31.5548	.245212
15.5000	1.05203	2.1672	.0154	121.4003	65.5138	31.2432	.254988
16.5000	1.04291	2.1728	.0127	139.1018	74.7560	30.9158	.262822
17.5000	1.03401	2.1783	.0100	159.7284	85.4751	30.5899	.268799
18.5000	1.02563	2.1835	.0076	183.5765	97.8133	30.2738	.273101
19.5000	1.01736	2.1886	.0051	211.9466	112.4267	29.9584	.275859
20.5000	1.00890	2.1940	.0026	246.9182	130.3589	29.6352	.277177
21.5000	1.00092	2.1991	.0003	289.0698	151.8799	29.3215	.277302
22.5000	.99316	2.2040	-.0020	341.6988	178.6378	29.0095	.276452
23.5000	.98538	2.2091	-.0043	410.5317	213.4864	28.6914	.274833
24.5000	.97797	2.2139	-.0065	501.5329	259.3719	28.3761	.272707
25.5000	.97155	2.2181	-.0084	619.9377	318.8651	28.0805	.270367
26.5000	.96475	2.2226	-.0104	798.0145	408.0062	27.7702	.268014
27.5000	.95829	2.2269	-.0123	1073.9261	545.6279	27.4625	.265893
28.5000	.95244	2.2308	-.0140	1534.3313	774.5263	27.1656	.264230
29.5000	.94683	2.2346	-.0157	2460.9632	1233.7786	26.8708	.263227
30.5000	.94115	2.2384	-.0174	5189.1350	2581.5988	26.5694	.263093
31.5000	.93605	2.2419	-.0189	34067.4106	16807.7049	26.2788	.263987
32.5000	.93121	2.2452	-.0203	*2658.9214	*1060.8293	25.9903	.266058
33.5000	.92636	2.2485	-.0217	-6264.6954	-3028.7916	25.6959	.269479
34.5000	.92185	2.2517	-.0231	-3437.1813	-1647.0495	25.4045	.274361
35.5000	.91830	2.2541	-.0241	-2378.9731	-1130.9714	25.1329	.280681
36.5000	.91444	2.2568	-.0253	-1777.1695	-838.1242	24.8471	.288593
37.5000	.91093	2.2593	-.0263	-1414.4816	-661.9880	24.5645	.298120
38.5000	.90809	2.2613	-.0271	-1181.3130	-548.9363	24.2934	.309183
39.5000	.90558	2.2630	-.0279	-1015.2246	-468.5248	24.0252	.321738
40.5000	.90309	2.2648	-.0286	-887.4902	-406.7710	23.7516	.335789
41.5000	.90125	2.2661	-.0291	-792.8251	-361.0532	23.4895	.351157
42.5000	.89975	2.2672	-.0296	-717.8015	-324.8526	23.2305	.367713
43.5000	.89829	2.2682	-.0300	-654.9294	-294.5410	22.9662	.385383
44.5000	.89721	2.2690	-.0303	-603.4036	-269.7151	22.7055	.403983
45.5000	.89710	2.2690	-.0304	-563.6214	-250.5486	22.4648	.423136
46.5000	.89674	2.2693	-.0305	-527.0375	-232.9267	22.2106	.442793
47.5000	.89680	2.2693	-.0305	-495.8912	-217.9235	21.9603	.462700
48.5000	.89760	2.2687	-.0302	-470.2125	-205.5484	21.7224	.482503
49.5000	.89883	2.2678	-.0299	-447.8936	-194.7846	21.4885	.501931

VISCOUS SOLUTION

X/L	THETA,FT	BODY-CF,LOCAL FLAT	PLATE CF,LOCAL	DEL STAR,FT	DELTA,FT
.00250	.00001322	.00467920	.00347823	.00004234	.00016715
.01250	.00005205	.00396972	.00322309	.00016679	.00066351
.03000	.00011052	.00348725	.00283543	.00035526	.00141481
.05000	.00017190	.00322033	.00262555	.00055459	.00220648
.07000	.00023040	.00304933	.00249651	.00074600	.00296303
.09000	.00028712	.00292387	.00240630	.00093298	.00369826
.11000	.00034262	.00282513	.00233726	.00111705	.00441882
.13000	.00039729	.00274246	.00228158	.00129995	.00513029
.15000	.00045144	.00267086	.00223510	.00148240	.00583615
.17000	.00050524	.00260815	.00219531	.00166484	.00653841
.19000	.00055885	.00255243	.00216059	.00184790	.00723914
.21000	.00061244	.00250111	.00212986	.00203239	.00794076
.23000	.00066612	.00245368	.00210234	.00221818	.00864398
.25000	.00071997	.00241038	.00207743	.00240558	.00934994
.27000	.00077415	.00236987	.00205471	.00259533	.01006067
.29000	.00082877	.00233093	.00203387	.00278750	.01077719
.31000	.00088387	.00229607	.00201460	.00298157	.01149899
.33000	.00093959	.00226351	.00199671	.00317944	.01222969
.35000	.00099607	.00223117	.00198003	.00338091	.01296997
.37000	.00105337	.00220080	.00196441	.00358581	.01372001
.39000	.00111159	.00217295	.00194973	.00379492	.01448152
.41000	.00117090	.00214525	.00193588	.00400931	.01525703
.43000	.00123138	.00211806	.00192279	.00422831	.01604618
.45000	.00129315	.00209289	.00191038	.00445265	.01685062
.47000	.00135641	.00206817	.00189858	.00468343	.01767307
.49000	.00142132	.00204205	.00188735	.00492060	.01851447
.51000	.00148792	.00201914	.00187663	.00516306	.01937344
.53000	.00155653	.00199795	.00186638	.00541436	.02025662
.55000	.00162737	.00197497	.00185657	.00567397	.02116451
.57000	.00170059	.00195311	.00184715	.00594179	.02209778
.59000	.00177646	.00193372	.00183810	.00621940	.02305979
.61000	.00185534	.00191353	.00182940	.00650889	.02405529
.63000	.00193748	.00189306	.00182102	.00680949	.02508433
.65000	.00202325	.00187500	.00181294	.00712320	.02615116
.67000	.00211315	.00185672	.00180513	.00745260	.02726165
.69000	.00220768	.00183527	.00179759	.00779833	.02841860
.71000	.00230718	.00181726	.00179029	.00815962	.02962197
.73000	.00241250	.00180126	.00178322	.00854331	.03088426
.75000	.00252442	.00178152	.00177637	.00894998	.03220894
.77000	.00264369	.00176237	.00176973	.00938103	.03359973
.79000	.00277136	.00174633	.00176328	.00984116	.03506568
.81000	.00290881	.00172848	.00175701	.01033631	.03661812
.83000	.00305740	.00170953	.00175091	.01086853	.03826203
.85000	.00321893	.00169396	.00174498	.01144524	.04000961
.87000	.00339580	.00167812	.00173921	.01207592	.04187622
.89000	.00359079	.00165649	.00173358	.01276855	.04387364
.91000	.00380694	.00164002	.00172810	.01353017	.04600892
.93000	.00404904	.00162747	.00172275	.01438348	.04830911
.95000	.00432277	.00160874	.00171753	.01534420	.05078633
.97000	.00463536	.00159196	.00171243	.01643445	.05345139
.99000	.00499670	.00106411	.00170962	.01768930	.05631745

BODY-CF,TOTAL= .00200549 FLAT-PLATE CF,TOTAL= .00189077

CD,WAVE= .03848177 CD,FRICTION= .07321805 CD,TOTAL= .11169982

RM 10 BODY

INPUT DATA ITERATION 2

M= 2.20
RN= 4.17000000E+06

X	Y	DELTA
.2500	.0340	7.5772
1.0000	.1337	7.5772
2.0000	.2627	7.3486
3.0000	.3872	7.0981
4.0000	.5073	6.8455
5.0000	.6229	6.5944
6.0000	.7343	6.3554
7.0000	.8412	6.1057
8.0000	.9438	5.8561
9.0000	1.0421	5.6124
10.0000	1.1360	5.3689
11.0000	1.2256	5.1197
12.0000	1.3109	4.8762
13.0000	1.3920	4.6327
14.0000	1.4686	4.3837
15.0000	1.5409	4.1344
16.0000	1.6090	3.8967
17.0000	1.6728	3.6481
18.0000	1.7322	3.3992
19.0000	1.7873	3.1561
20.0000	1.8382	2.9135
21.0000	1.8848	2.6651
22.0000	1.9271	2.4224
23.0000	1.9652	2.1802
24.0000	1.9989	1.9325
25.0000	2.0283	1.6844
26.0000	2.0536	1.4484
27.0000	2.0746	1.2019
28.0000	2.0912	.9550
29.0000	2.1037	.7144
30.0000	2.1120	.4748
31.0000	2.1160	.2299
32.0000	2.1158	-.0090
33.0000	2.1115	-.2464
34.0000	2.1030	-.4887
35.0000	2.0903	-.7310
36.0000	2.0735	-.9601
37.0000	2.0526	-1.1984
38.0000	2.0275	-1.4363
39.0000	1.9984	-1.6667
40.0000	1.9653	-1.8940
41.0000	1.9282	-2.1249
42.0000	1.8872	-2.3476
43.0000	1.8424	-2.5657
44.0000	1.7938	-2.7850
45.0000	1.7414	-3.0010
46.0000	1.6855	-3.1982
47.0000	1.6261	-3.3976
48.0000	1.5634	-3.5892
49.0000	1.4976	-3.7633
50.0000	1.4280	-3.9830

STARTING CONE – M= 2.07391 THETA= 28.003 DELSOR= .0000

OUTPUT

INVISCID SOLUTION

X,IN	P/P(INF)	M	CP	X-SHOCK	Y-SHOCK	CHARACTERISTIC ANGLE	D/Q,SQ IN
.1250	1.21727	2.0739	.0641	.7452	.3991	36.4051	.000221
1ST ORDER SHOCK EXPANSION							
.6250	1.21727	2.0739	.0641	3.4495	1.9400	36.4051	.003447
1.5000	1.20642	2.0797	.0609	7.2787	4.1105	36.0895	.012844
2.5000	1.19412	2.0862	.0573	11.4037	6.4349	35.7402	.026851
3.5000	1.18245	2.0925	.0539	15.8461	8.9239	35.3937	.044326
4.5000	1.17105	2.0987	.0505	20.6422	11.5962	35.0504	.064254
5.5000	1.16042	2.1045	.0473	25.7831	14.4457	34.7254	.085869
6.5000	1.14912	2.1108	.0440	31.4263	17.5562	34.3839	.108252
7.5000	1.13798	2.1170	.0407	37.5866	20.9330	34.0436	.130729
8.5000	1.12727	2.1231	.0376	44.2835	24.5843	33.7124	.152803
9.5000	1.11663	2.1292	.0344	51.6422	28.5750	33.3818	.173992
10.5000	1.10568	2.1355	.0312	59.8560	33.0049	33.0427	.193806
11.5000	1.09522	2.1415	.0281	68.8852	37.8487	32.7129	.212030
12.5000	1.08499	2.1475	.0251	78.9395	43.2143	32.3850	.228461
13.5000	1.07480	2.1536	.0221	90.3357	49.2641	32.0516	.242905
14.5000	1.06501	2.1594	.0192	103.2005	56.0591	31.7209	.255325
15.5000	1.05626	2.1647	.0166	117.3527	63.5000	31.4103	.265895
16.5000	1.04707	2.1703	.0139	134.0140	72.2182	31.0849	.274488
17.5000	1.03812	2.1758	.0113	153.2984	82.2615	30.7610	.281186
18.5000	1.02972	2.1810	.0088	175.4076	93.7250	30.4473	.286174
19.5000	1.02149	2.1861	.0063	201.4188	107.1527	30.1353	.289583
20.5000	1.01303	2.1914	.0038	233.1194	123.4436	29.8156	.291513
21.5000	1.00506	2.1964	.0015	270.8507	142.7509	29.5054	.292204
22.5000	.99728	2.2014	-.0008	317.2018	166.3695	29.1971	.291865
23.5000	.98944	2.2065	-.0031	376.6586	196.5378	28.8827	.290696
24.5000	.98191	2.2113	-.0053	453.5457	235.3904	28.5702	.288951
25.5000	.97539	2.2156	-.0073	550.3505	284.1334	28.2785	.286927
26.5000	.96855	2.2201	-.0093	689.4691	353.9190	27.9732	.284827
27.5000	.96201	2.2244	-.0112	892.7817	455.5385	27.6702	.282895
28.5000	.95610	2.2284	-.0130	1202.6105	609.8897	27.3786	.281360
29.5000	.95049	2.2321	-.0146	1737.4932	875.5278	27.0906	.280426
30.5000	.94482	2.2359	-.0163	2889.6385	1445.9035	26.7966	.280301
31.5000	.93972	2.2394	-.0178	6363.0721	3160.5373	26.5135	.281143
32.5000	.93490	2.2427	-.0192	84627.1568	41690.3154	26.2342	.283104
33.5000	.93006	2.2460	-.0206	*6249.5759	*7655.2258	25.9498	.286352
34.5000	.92551	2.2491	-.0220	*2140.1962	-5848.9846	25.6677	.291006
35.5000	.92197	2.2516	-.0230	-7228.2274	-3448.4424	25.4078	.297042
36.5000	.91819	2.2542	-.0241	-4974.0266	-2349.1607	25.1363	.304607
37.5000	.91472	2.2566	-.0252	-3763.5372	-1760.0202	24.8682	.313728
38.5000	.91197	2.2586	-.0260	-3044.5403	-1410.6392	24.6136	.324325
39.5000	.90962	2.2602	-.0267	-2561.9867	-1176.4680	24.3657	.336343
40.5000	.90734	2.2618	-.0273	-2204.7136	-1003.3193	24.1147	.349777
41.5000	.90576	2.2629	-.0278	-1948.7660	-879.3893	23.8781	.364443
42.5000	.90464	2.2637	-.0281	-1753.5097	-784.9071	23.6502	.380190
43.5000	.90367	2.2644	-.0284	-1594.4185	-707.9681	23.4222	.396926
44.5000	.90309	2.2648	-.0286	-1466.4897	-646.1202	23.2012	.414462
45.5000	.90372	2.2644	-.0284	-1373.3165	-601.0587	23.0096	.432383
46.5000	.90433	2.2639	-.0282	-1291.1833	-561.3225	22.8156	.450593
47.5000	.90550	2.2631	-.0279	-1224.1866	-528.8876	22.6342	.468822
48.5000	.90768	2.2616	-.0273	-1174.0993	-504.6086	22.4793	.486677
49.5000	.90751	2.2617	-.0273	-1107.2445	-472.2049	22.2581	.504437

VISCOUS SOLUTION

X/L	THETA,FT	BODY-CF,LOCAL FLAT	PLATE CF,LOCAL	DEL STAR,FT	DELTA,FT
.00250	.00001323	.00469244	.00347699	.00004228	.00016717
.01250	.00005210	.00398097	.00322194	.00016659	.00066362
.03000	.00011062	.00349524	.00283449	.00035489	.00141508
.05000	.00017203	.00322666	.00262477	.00055405	.00220683
.07000	.00023057	.00305475	.00249583	.00074525	.00296335
.09000	.00028732	.00292901	.00240568	.00093198	.00369851
.11000	.00034284	.00282925	.00233669	.00111580	.00441898
.13000	.00039754	.00274658	.00228105	.00129838	.00513025
.15000	.00045171	.00267488	.00223461	.00148052	.00583590
.17000	.00050554	.00261171	.00219485	.00166262	.00653792
.19000	.00055918	.00255549	.00216015	.00184529	.00723832
.21000	.00061278	.00250456	.00212944	.00202933	.00793950
.23000	.00066648	.00245701	.00210194	.00221473	.00864238
.25000	.00072036	.00241337	.00207705	.00240183	.00934811
.27000	.00077456	.00237289	.00205436	.00259123	.01005854
.29000	.00082920	.00233439	.00203353	.00278313	.01077484
.31000	.00088432	.00229778	.00201429	.00297701	.01149656
.33000	.00094004	.00226543	.00199641	.00317431	.01222657
.35000	.00099653	.00223335	.00197975	.00337533	.01296633
.37000	.00105384	.00220239	.00196415	.00357981	.01371594
.39000	.00111207	.00217380	.00194948	.00378832	.01447671
.41000	.00117137	.00214683	.00193565	.00400190	.01525116
.43000	.00123186	.00211946	.00192258	.00422037	.01603968
.45000	.00129364	.00209389	.00191018	.00444409	.01684336
.47000	.00135689	.00206967	.00189841	.00467415	.01766490
.49000	.00142181	.00204485	.00188720	.00491089	.01850585
.51000	.00148845	.00201986	.00187649	.00515342	.01936518
.53000	.00155704	.00199903	.00186626	.00540372	.02024699
.55000	.00162788	.00197690	.00185647	.00566284	.02115436
.57000	.00170113	.00195451	.00184708	.00593047	.02208757
.59000	.00177700	.00193403	.00183805	.00620746	.02304887
.61000	.00185586	.00191494	.00182937	.00649584	.02404287
.63000	.00193802	.00189437	.00182102	.00679612	.02507172
.65000	.00202379	.00187542	.00181296	.00710910	.02613772
.67000	.00211367	.00185783	.00180519	.00743728	.02724663
.69000	.00220821	.00183878	.00179768	.00778245	.02840309
.71000	.00230778	.00181799	.00179041	.00814440	.02960794
.73000	.00241306	.00180221	.00178339	.00852609	.03086755
.75000	.00252499	.00178455	.00177658	.00893202	.03219158
.77000	.00264431	.00176500	.00176998	.00936313	.03358305
.79000	.00277200	.00174720	.00176358	.00982232	.03504818
.81000	.00290941	.00173115	.00175737	.01031527	.03659799
.83000	.00305805	.00171225	.00175134	.01084704	.03824205
.85000	.00321958	.00169442	.00174549	.01142187	.03998779
.87000	.00339636	.00167904	.00173981	.01204882	.04185004
.89000	.00359131	.00166161	.00173428	.01273842	.04384447
.91000	.00380756	.00163933	.00172891	.01349937	.04598047
.93000	.00404939	.00162515	.00172371	.01434410	.04827087
.95000	.00432296	.00160982	.00171865	.01529773	.05074130
.97000	.00463544	.00159164	.00171375	.01638138	.05340133
.99000	.00499657	.00107464	.00171112	.01762698	.05626034

BODY-CF,TOTAL= .00200748 FLAT-PLATE CF,TOTAL= .00189082

CD,WAVE= .03867395 CD,FRICTION= .07329059 CD,TOTAL= .11196454

REFERENCES

1. Jones, Robert T.: Theory of Wing-Body Drag at Supersonic Speeds. NACA Rep. 1284, 1956. (Supersedes NACA RM A53H18a.)

2. Sommer, Simon C.; and Short, Barbara J.: Free-Flight Measurements of Skin Friction of Turbulent Boundary Layers with High Rates of Heat Transfer at High Supersonic Speeds. J. Aeronaut. Sci., vol. 23, no. 6, June 1956, pp. 536-542.

3. Syvertson, Clarence A.; and Dennis, David H.: A Second-Order Shock-Expansion Method Applicable to Bodies of Revolution Near Zero Lift. NACA Rep. 1328, 1957. (Supersedes NACA TN 3527.)

4. Savin, Raymond C.: Application of the Generalized Shock-Expansion Method to Inclined Bodies of Revolution Traveling at High Supersonic Airspeeds. NACA TN 3349, 1955.

5. Englert, Gerald W.: Estimation of Compressible Boundary-Layer Growth Over Insulated Surfaces With Pressure Gradient. NACA TN 4022, 1957.

6. Reshotko, Eli; and Tucker, Maurice: Approximate Calculation of the Compressible Turbulent Boundary Layer With Heat Transfer and Arbitrary Pressure Gradient. NACA TN 4154, 1957.

7. Sims, Joseph L.: Tables for Supersonic Flow Around Right Circular Cones at Zero Angle of Attack. NASA SP-3004, 1964.

8. Truckenbrodt, E.: A Method of Quadrature for Calculation of the Laminar and Turbulent Boundary Layer in Case of Plane and Rotationally Symmetrical Flow. NACA TM 1379, 1955.

9. Stewartson, K.: Correlated Incompressible and Compressible Boundary Layers. Proc. Roy. Soc. (London), ser. A, vol. 200, no. A1060, Dec. 22, 1949, pp. 84-100.

10. Allen, Jerry M.; and Monta, William J.: Turbulent-Boundary-Layer Characteristics of Pointed Slender Bodies of Revolution at Supersonic Speeds. NASA TN D-4193, 1967.

11. Czarnecki, K. R.; and Monta, William J.: Boundary-Layer Velocity Profiles and Skin Friction Due to Surface Roughness on an Ogive Cylinder at Mach Numbers of 1.61 and 2.01. NASA TN D-2048, 1963.

12. Adcock, Jerry B.; Peterson, John B., Jr.; and McRee, Donald I.: Experimental Investigation of a Turbulent Boundary Layer at Mach 6, High Reynolds Numbers, and Zero Heat Transfer. NASA TN D-2907, 1965.

13. Tucker, Maurice: Approximate Turbulent Boundary-Layer Development in Plane Compressible Flow Along Thermally Insulated Surfaces With Application to Supersonic-Tunnel Contour Correction. NACA TN 2045, 1950.

14. Probstein, Ronald F.; and Elliott, David: The Transverse Curvature Effect in Compressible Axially Symmetric Laminar Boundary-Layer Flow. J. Aeronaut. Sci., vol. 23, no. 3, Mar. 1956, pp. 208-224, 236.

15. Hasel, Lowell E.; Sinclair, Archibald R.; and Hamilton, Clyde V.: Preliminary Investigation of the Drag Characteristics of the NACA RM-10 Missile at Mach Numbers of 1.40 and 1.59 in the Langley 4- by 4-Foot Supersonic Tunnel. NACA RM L52A14, 1952.

16. Winter, K. G.; Smith, K. G.; and Rotta, J. C.: Turbulent Boundary-Layer Studies on a Waisted Body of Revolution in Subsonic and Supersonic Flow. Recent Developments in Boundary Layer Research, Pt. II, AGARDograph 97, May 1965, pp. 933-961.

17. Harris, Roy V., Jr.; and Landrum, Emma Jean: Drag Characteristics of a Series of Low-Drag Bodies of Revolution at Mach Numbers From 0.6 to 4.0. NASA TN D-3163, 1965.

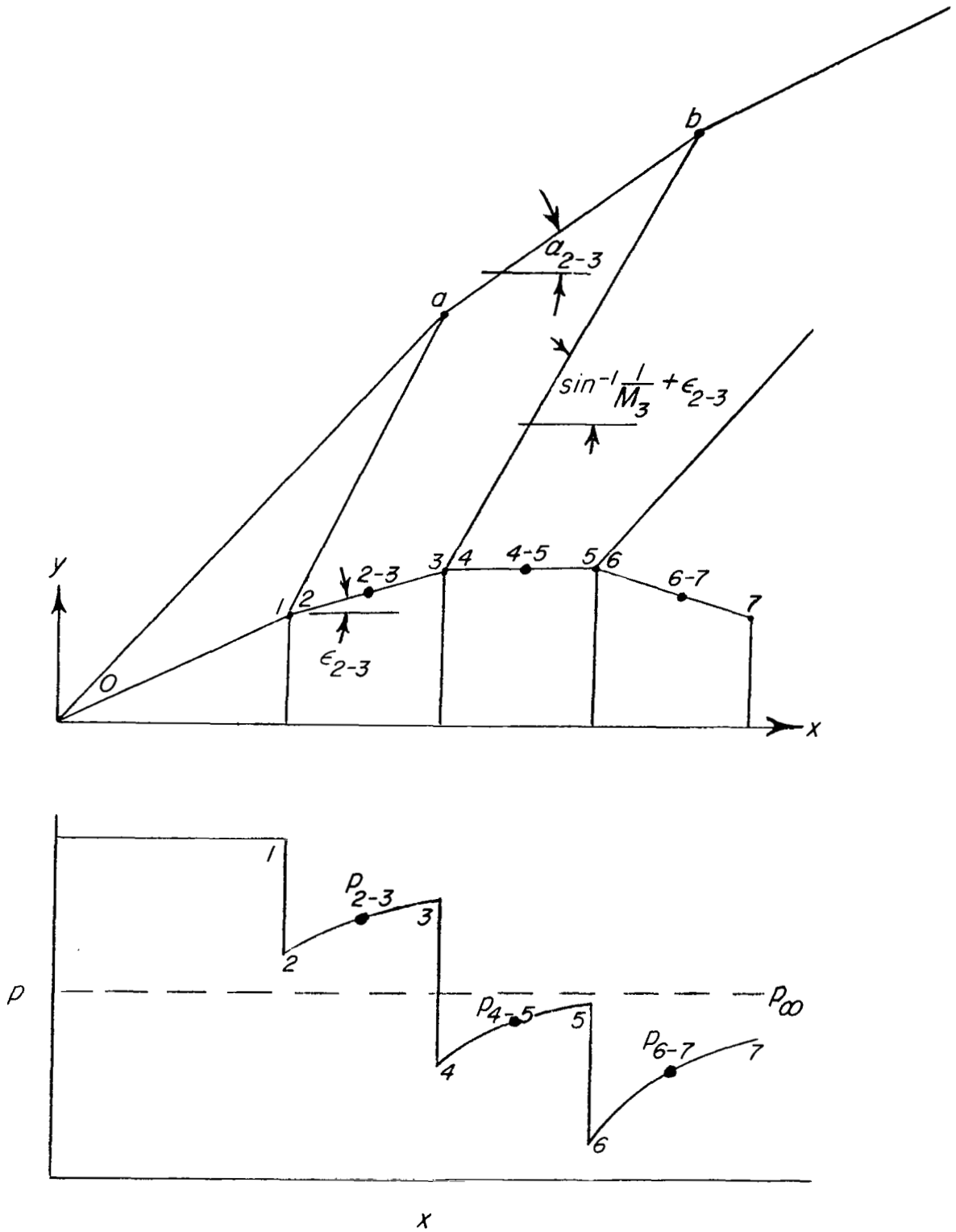

Figure 1.- Method of application for inviscid solution.

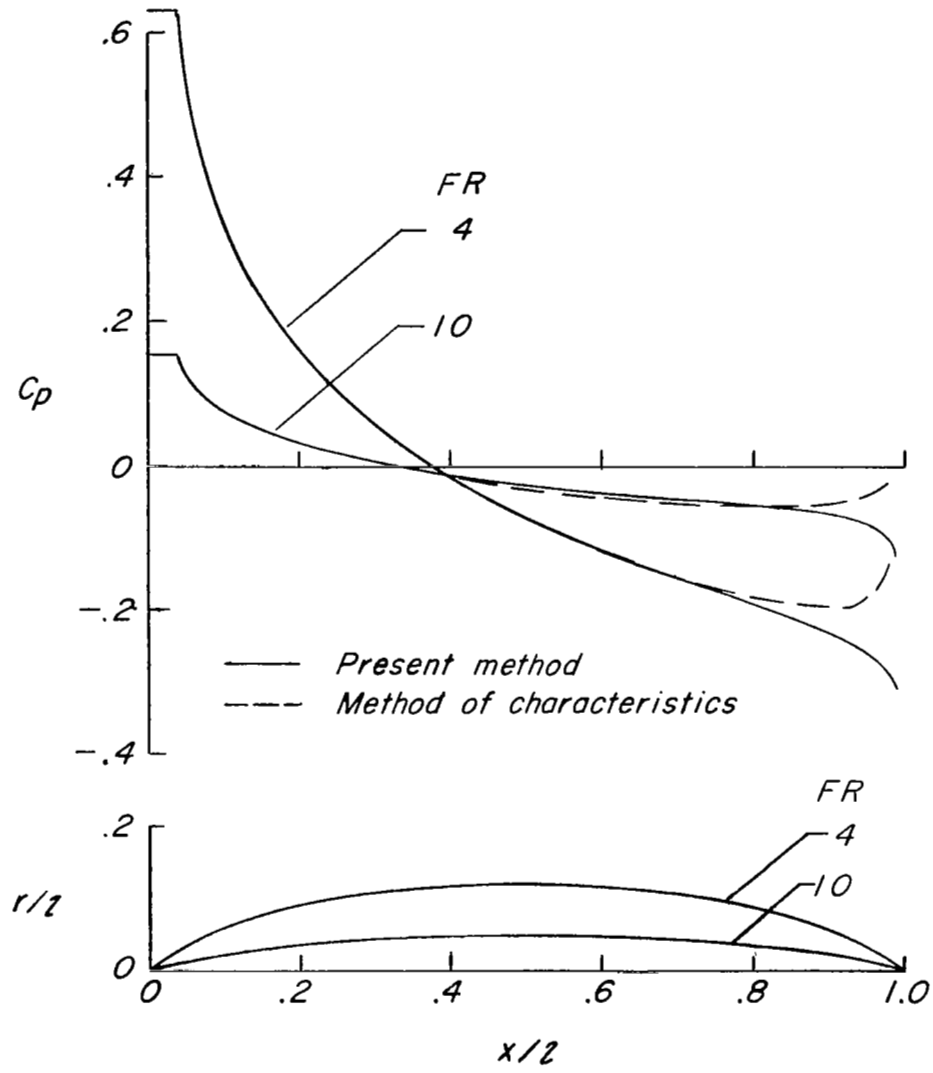

Figure 2.- Comparison of surface-pressure-coefficient distributions computed for typical boattail bodies (Sears-Haack bodies) by the present method and method of characteristics. $M_\infty = 2.0$.

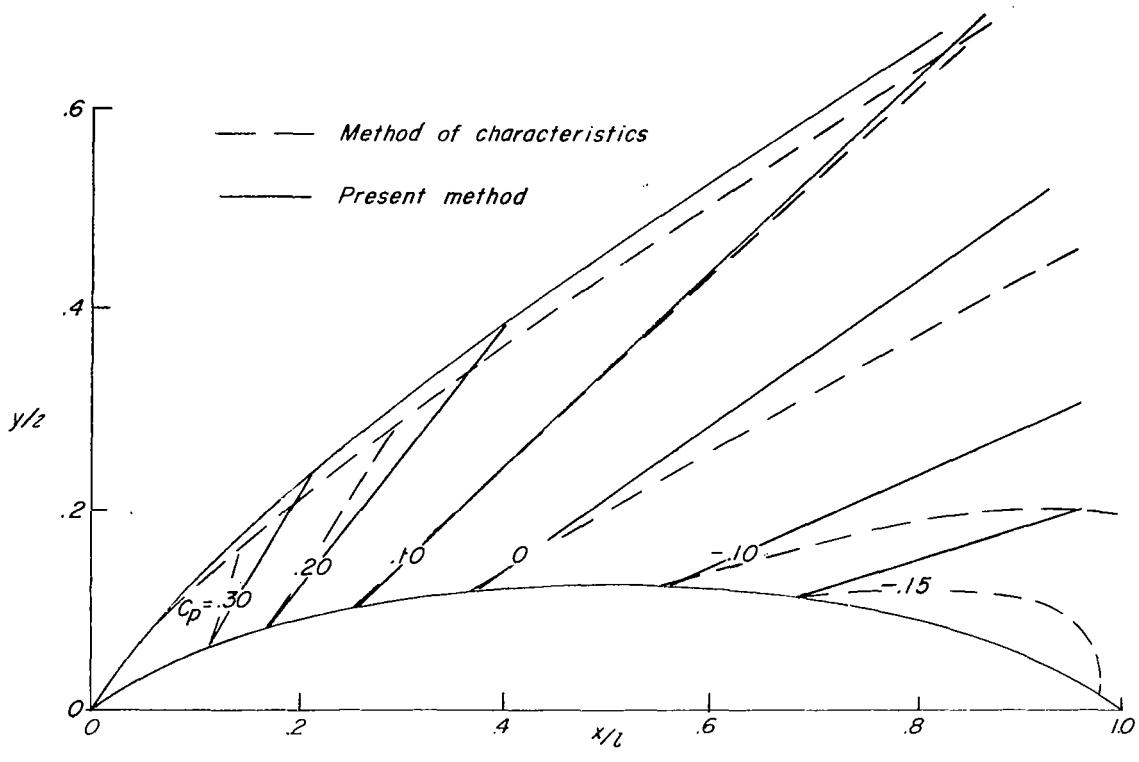

(a) FR = 4.

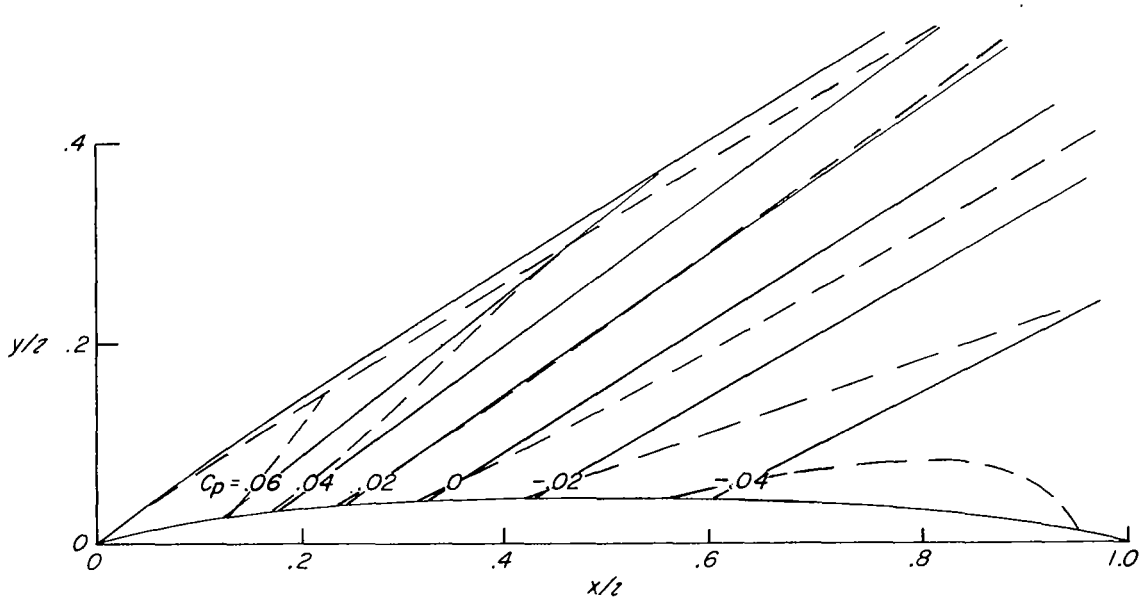

(b) FR = 10.

Figure 3.- Comparison of pressure coefficients and shock shape obtained from the present theoretical method and the method of characteristics for the flow fields about Sears-Haack bodies at M_∞ = 2.0.

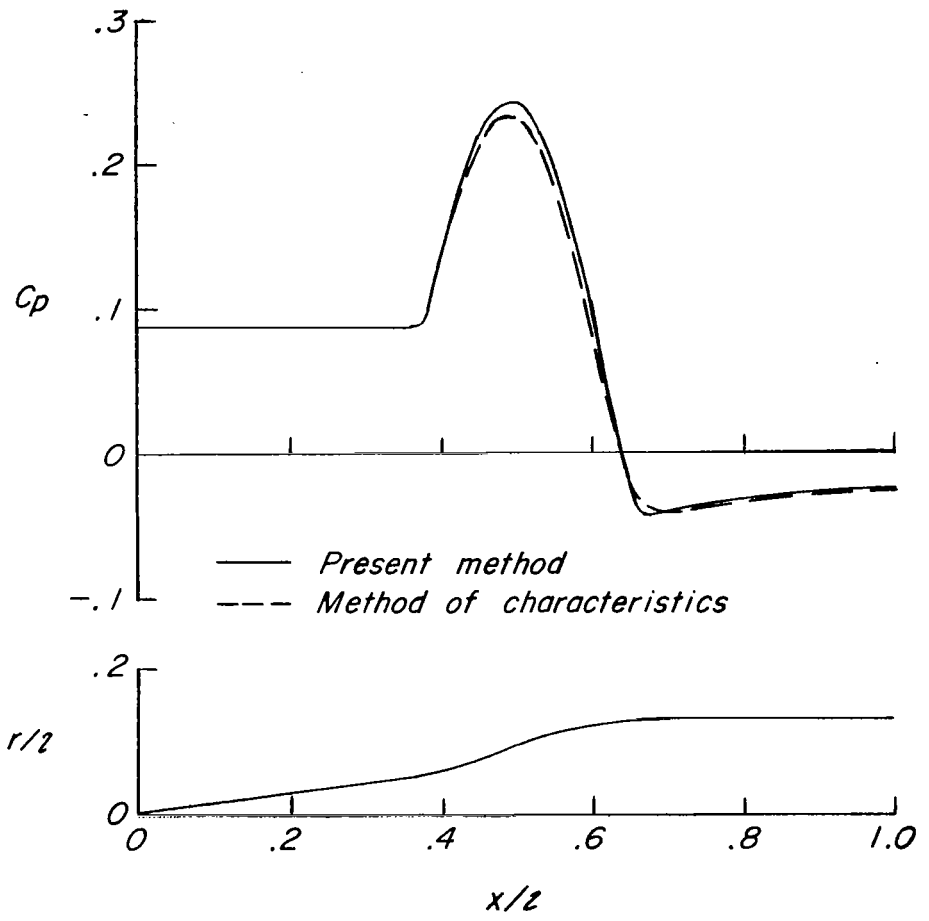

Figure 4.- Comparison of the present theoretical method with the method of characteristics for obtaining surface-pressure coefficients on an inlet spike with compression and expansion flow at $M_\infty = 3.0$.

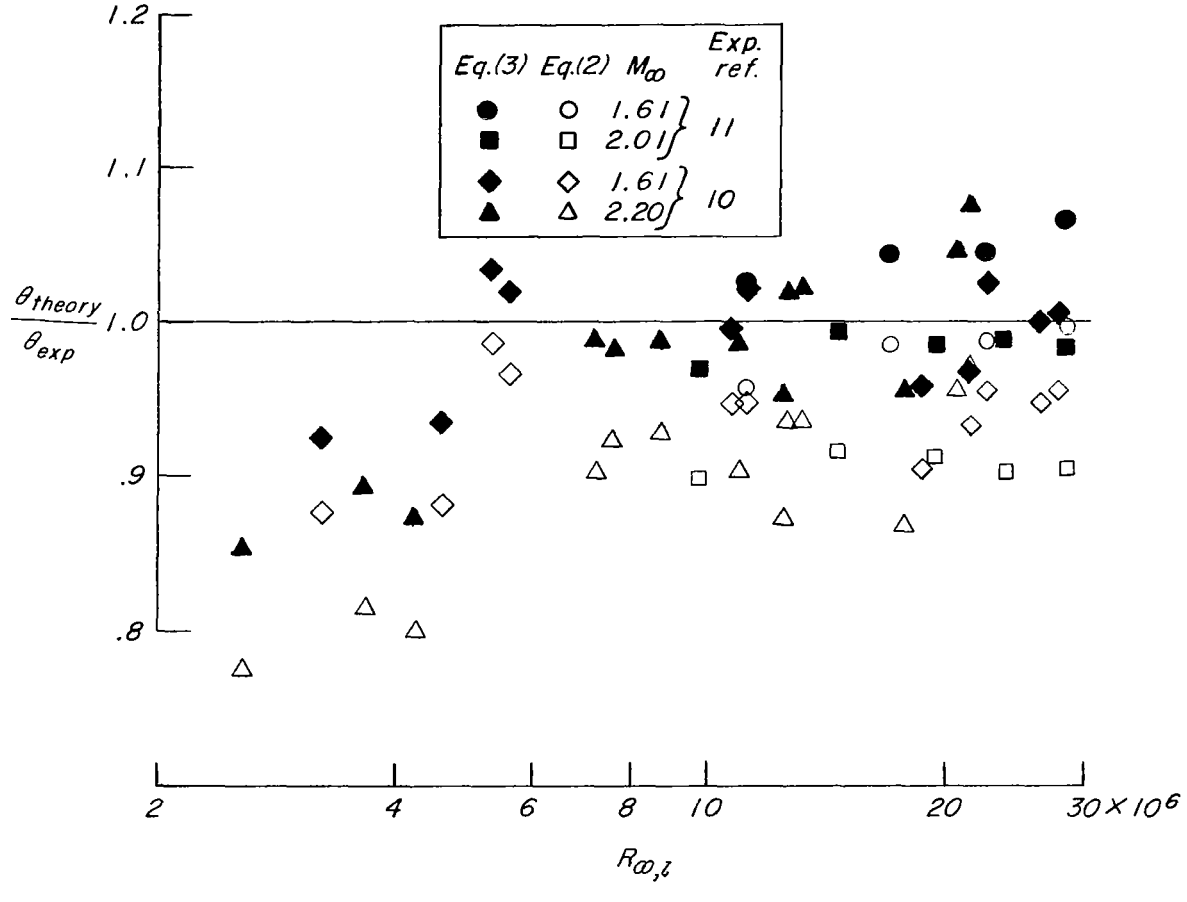

Figure 5.- Comparison of the theoretical methods of reference 5 (eq. (2)) with the present theory (eq. (3)) for estimating the momentum thickness of a turbulent boundary layer.

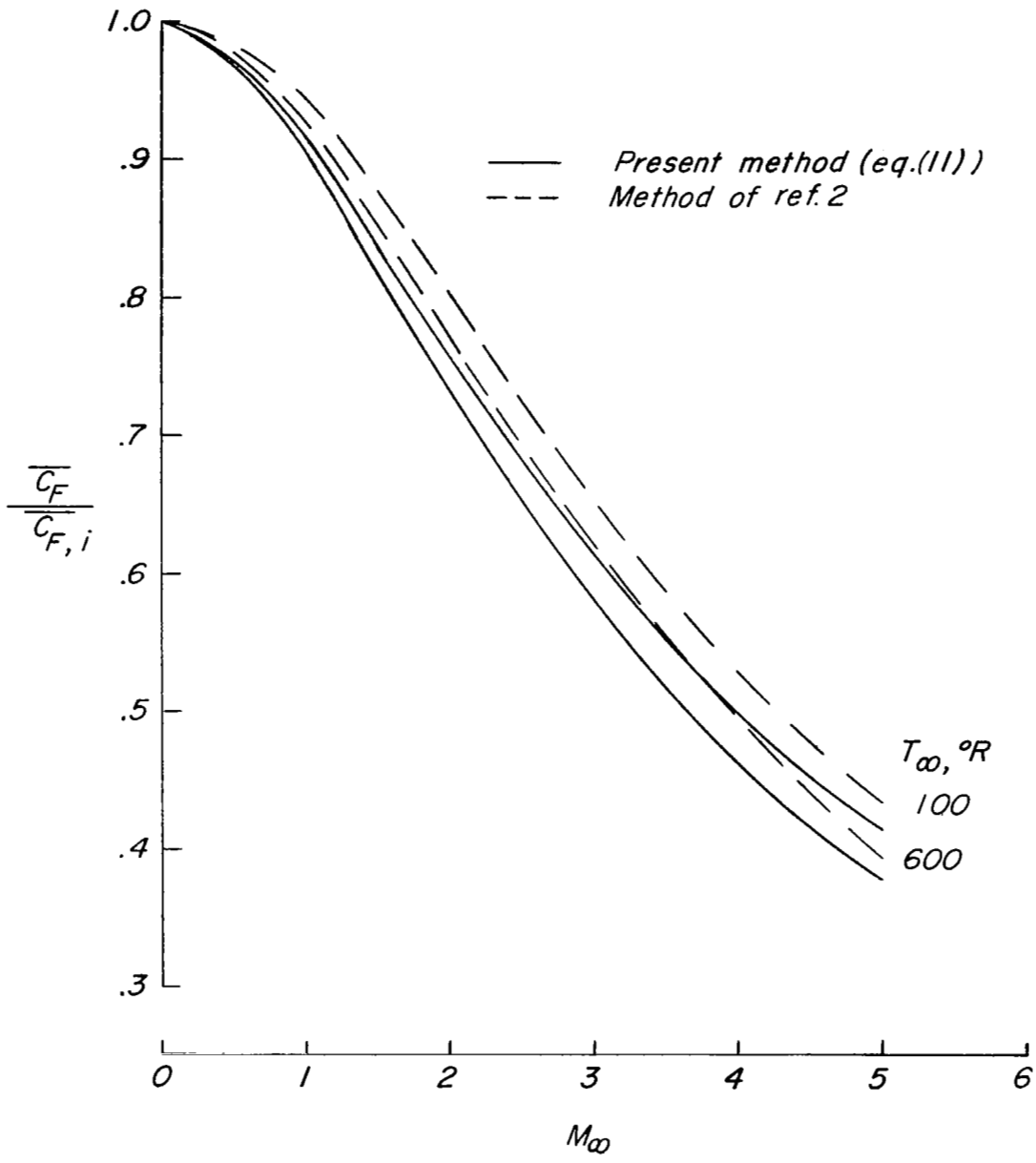

Figure 6.- Comparison of the compressibility factor of the present analysis with that obtained by the method of reference 2. (For the method of reference 2, the Kármán-Schoenherr incompressible skin-friction law was used with $R_{\infty,l} = 10 \times 10^6$.)

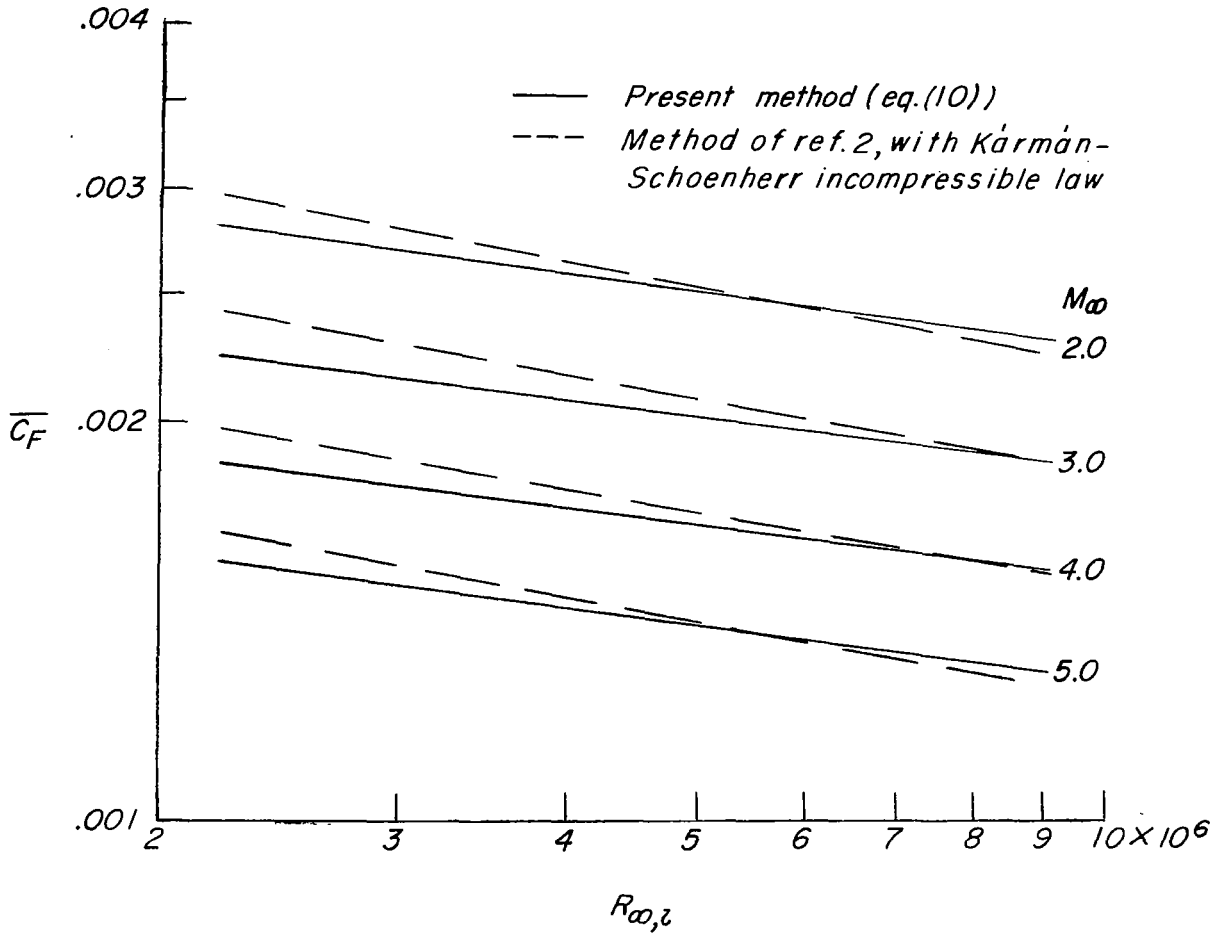

Figure 7.- Comparison of values of $\overline{C_F}$ obtained by the method of the present analysis with those obtained by the method of reference 2 and the Kármán-Schoenherr incompressible law. $T_t = 600^0$ R.

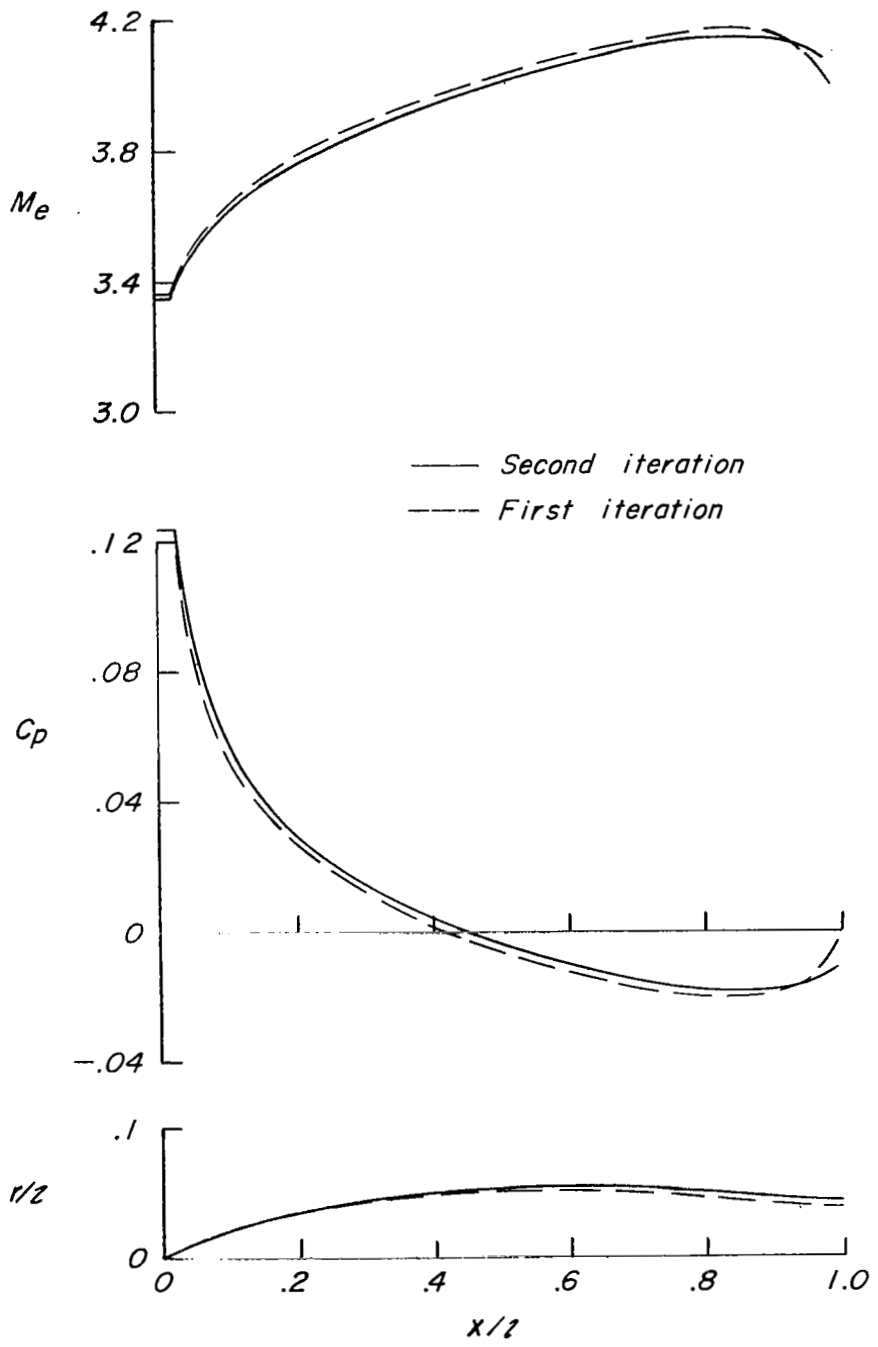

(a) Inviscid solution.

Figure 8.- Typical results of the present method applied to an Adam's body of FR = 10 and $\frac{A_{max}}{A_{base}} = 1.88$ at $M_\infty = 4.0$ and $R_{\infty,l} = 9.0 \times 10^6$.

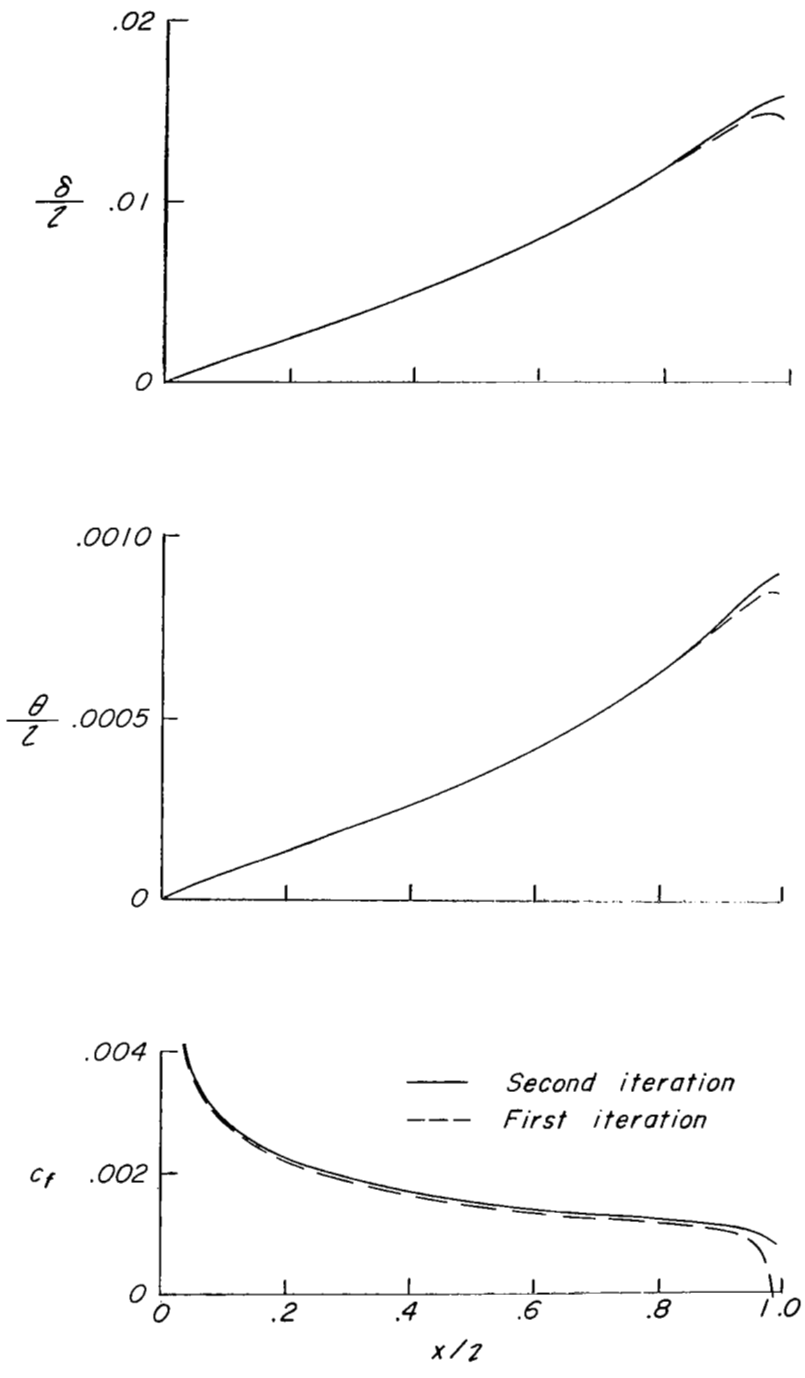

(b) Viscid solution.

Figure 8.- Concluded.

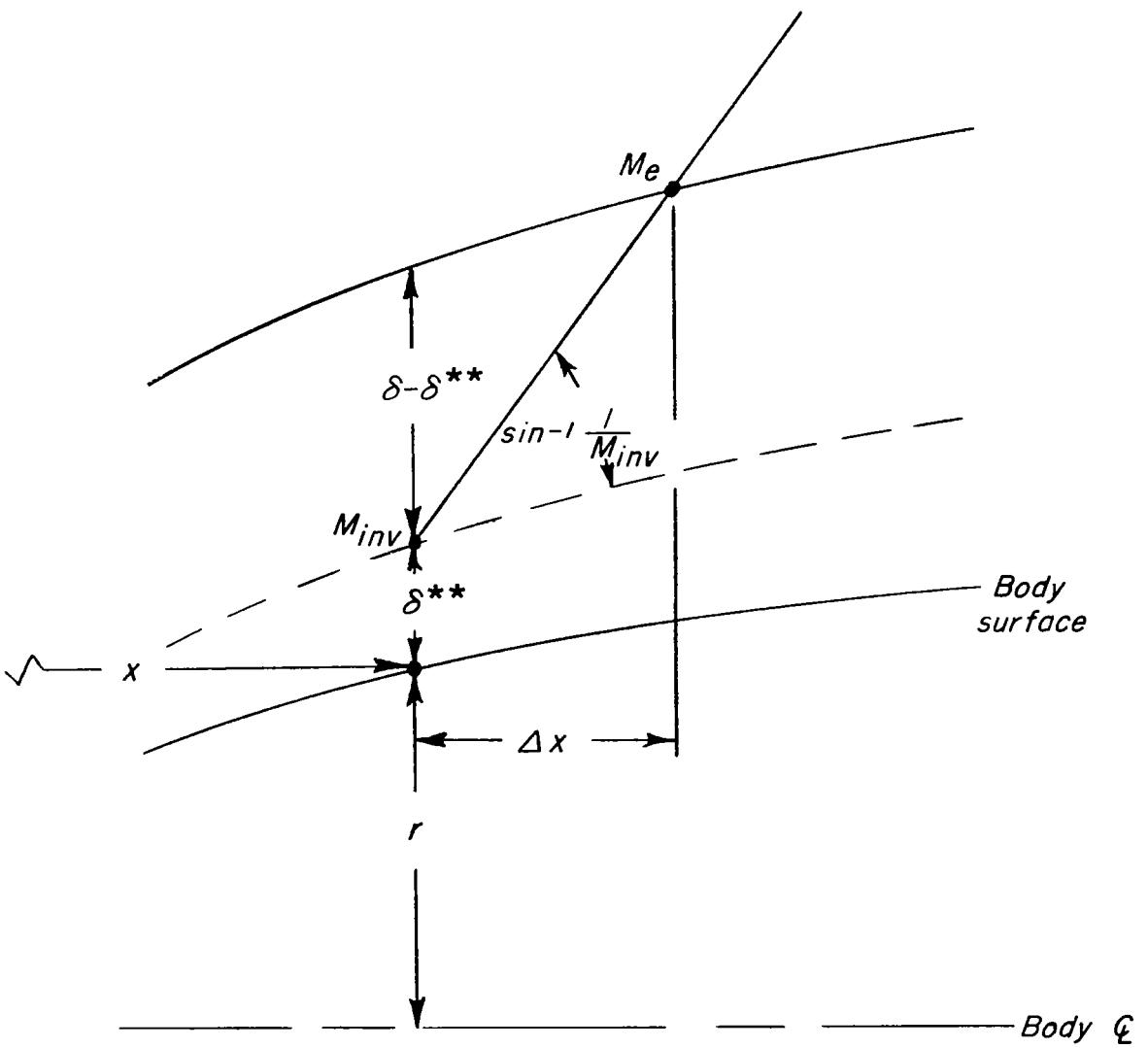

Figure 9.- Geometry used for correcting inviscid parameters to boundary-layer edge conditions.

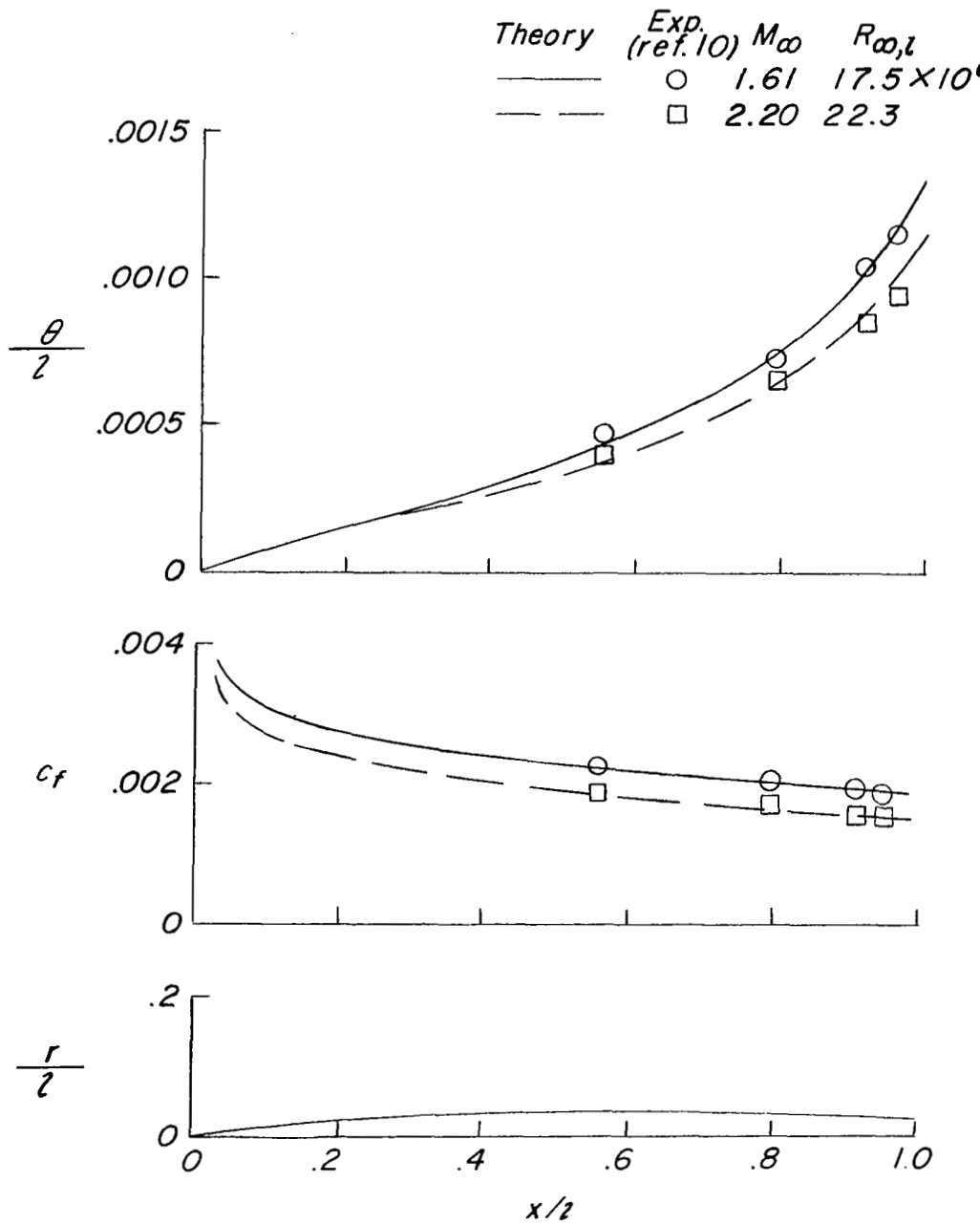

Figure 10.- Variation of momentum thickness and local skin-friction coefficient on NACA RM-10 missile body.

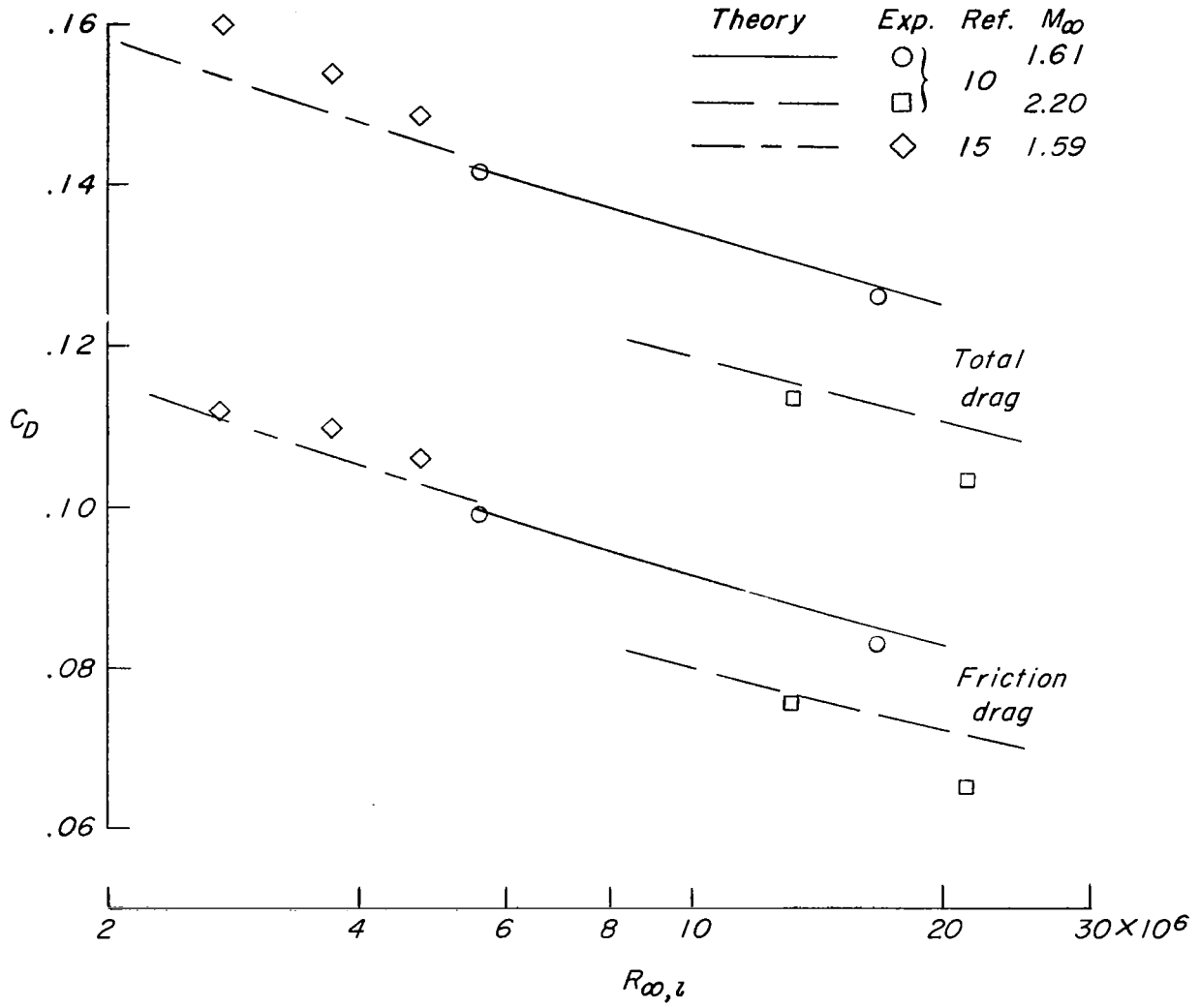

Figure 11.- Comparison of theoretical and experimental friction-drag and total-drag coefficients for NACA RM-10 missile body.

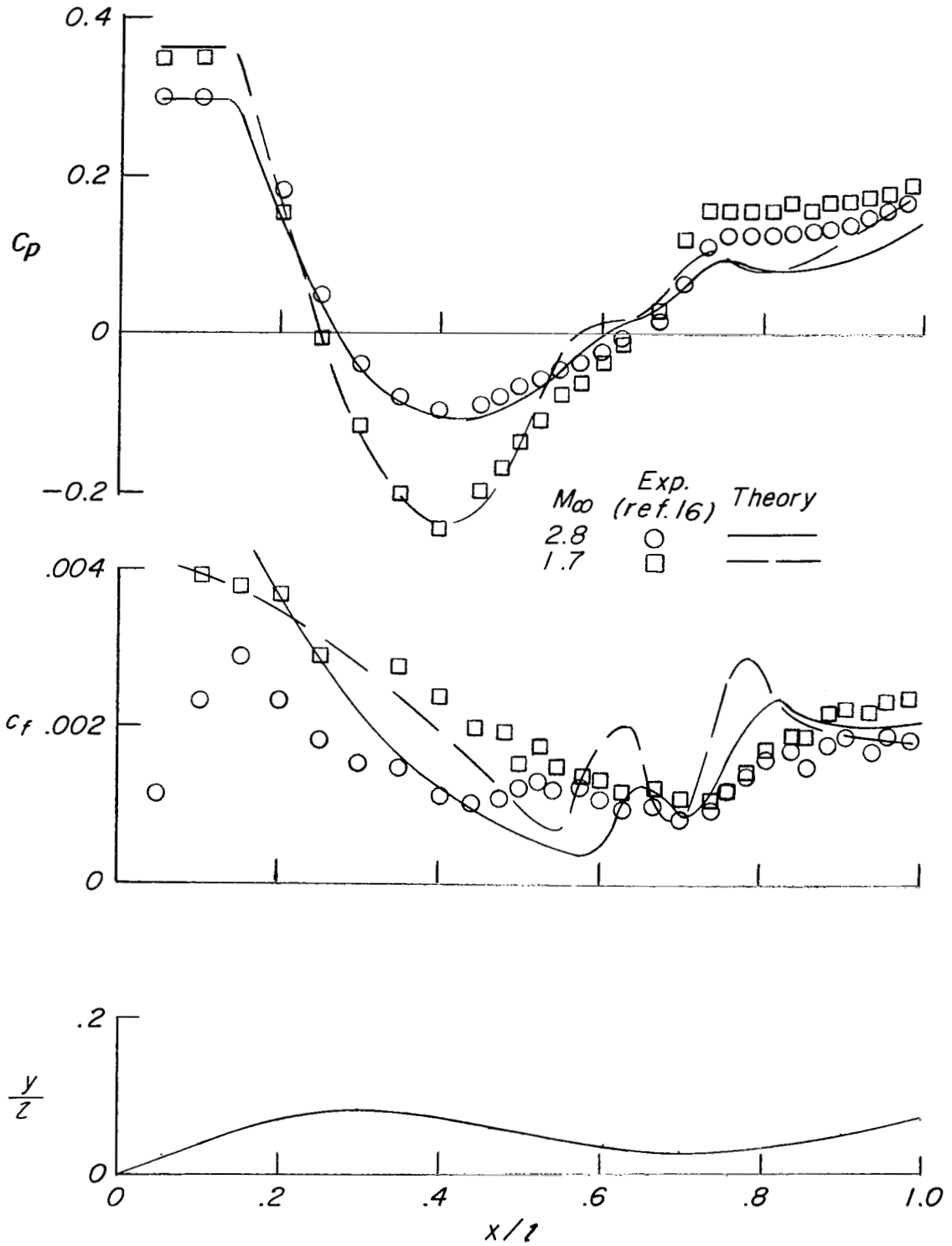

Figure 12.- Comparison of experimental and theoretical surface-pressure coefficients and local skin-friction coefficients for a waisted body of revolution. $R_{\infty,l} = 10 \times 10^6$.

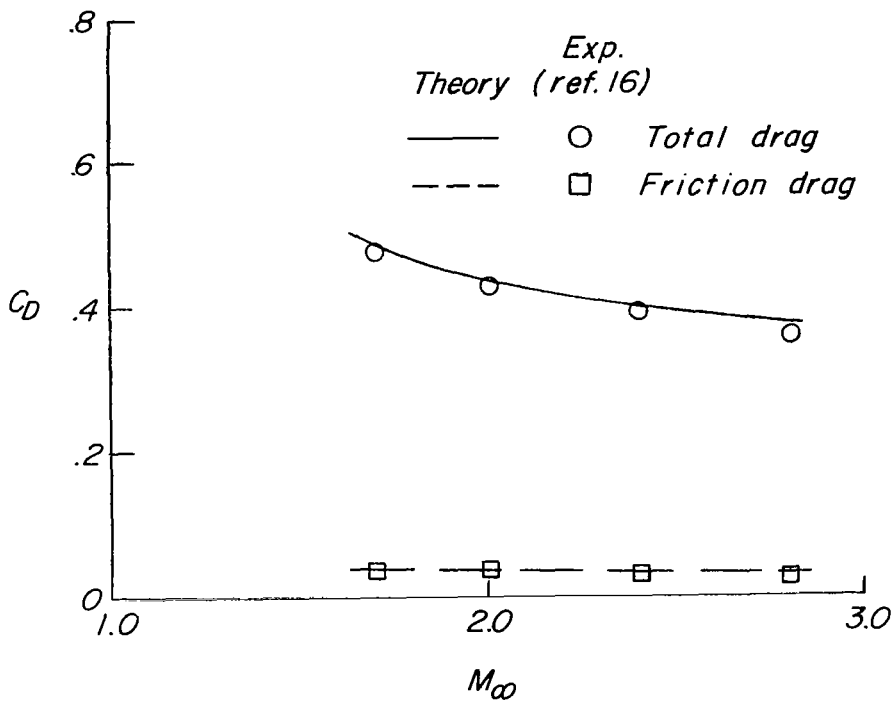

Figure 13.- Comparison of theoretical and experimental friction-drag and total-drag coefficients for the waisted body. $R_{\infty,l} = 10 \times 10^6$.

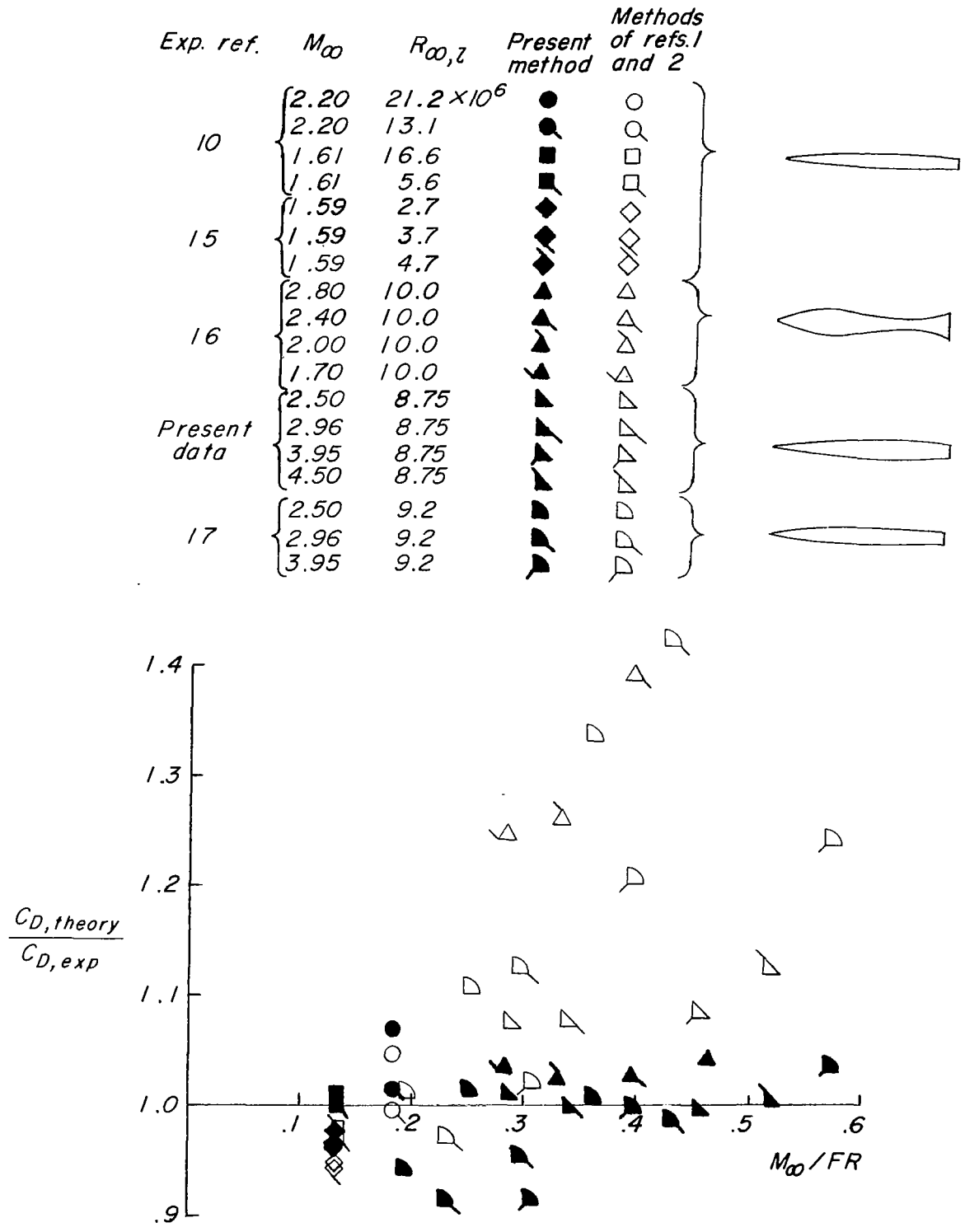

Figure 14.- Evaluation of theoretical total-drag predictions.

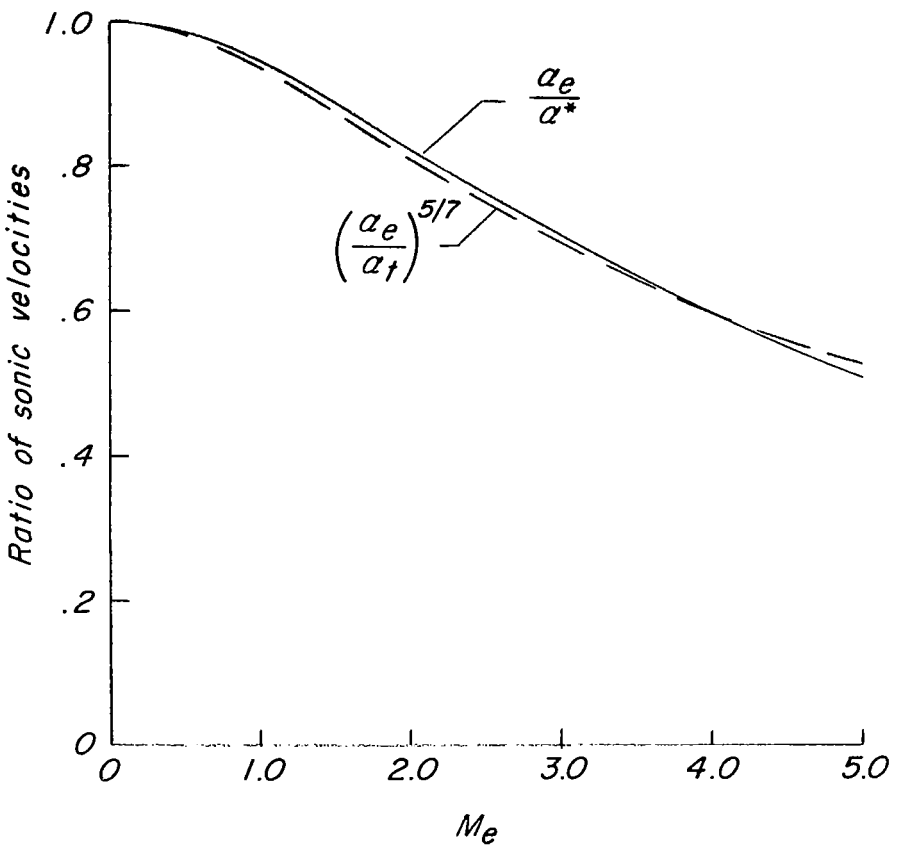

Figure 15.- Comparison of sonic velocity ratio based on reference temperature with that based on stagnation temperature.

NATIONAL AERONAUTICS AND SPACE ADMINISTRATION
WASHINGTON, D.C. 20546
OFFICIAL BUSINESS

FIRST CLASS MAIL

POSTAGE AND FEES PAID
NATIONAL AERONAUTICS AN
SPACE ADMINISTRATION

050 001 26 51 3DS 69058 00903
AIR FORCE WEAPONS LABORATORY/AFWL/
KIRTLAND AIR FORCE BASE, NEW MEXICO 8711

ATT E. LOU BOWMAN, ACTING CHIEF TECH. LI

POSTMASTER: If Undeliverable (Section 15. Postal Manual) Do Not Retu

"The aeronautical and space activities of the United States shall be conducted so as to contribute . . . to the expansion of human knowledge of phenomena in the atmosphere and space. The Administration shall provide for the widest practicable and appropriate dissemination of information concerning its activities and the results thereof."

—NATIONAL AERONAUTICS AND SPACE ACT OF 1958

NASA SCIENTIFIC AND TECHNICAL PUBLICATIONS

TECHNICAL REPORTS: Scientific and technical information considered important, complete, and a lasting contribution to existing knowledge.

TECHNICAL NOTES: Information less broad in scope but nevertheless of importance as a contribution to existing knowledge.

TECHNICAL MEMORANDUMS: Information receiving limited distribution because of preliminary data, security classification, or other reasons.

CONTRACTOR REPORTS: Scientific and technical information generated under a NASA contract or grant and considered an important contribution to existing knowledge.

TECHNICAL TRANSLATIONS: Information published in a foreign language considered to merit NASA distribution in English.

SPECIAL PUBLICATIONS: Information derived from or of value to NASA activities. Publications include conference proceedings, monographs, data compilations, handbooks, sourcebooks, and special bibliographies.

TECHNOLOGY UTILIZATION PUBLICATIONS: Information on technology used by NASA that may be of particular interest in commercial and other non-aerospace applications. Publications include Tech Briefs, Technology Utilization Reports and Notes, and Technology Surveys.

Details on the availability of these publications may be obtained from:

SCIENTIFIC AND TECHNICAL INFORMATION DIVISION

NATIONAL AERONAUTICS AND SPACE ADMINISTRATION

Washington, D.C. 20546